

1-1-2011

Numerical simulation of a fuel nozzle's spray

Ashley Ann Marie Fergusson
Ryerson University

Follow this and additional works at: <http://digitalcommons.ryerson.ca/dissertations>



Part of the [Aerospace Engineering Commons](#)

Recommended Citation

Fergusson, Ashley Ann Marie, "Numerical simulation of a fuel nozzle's spray" (2011). *Theses and dissertations*. Paper 881.

This Thesis is brought to you for free and open access by Digital Commons @ Ryerson. It has been accepted for inclusion in Theses and dissertations by an authorized administrator of Digital Commons @ Ryerson. For more information, please contact bcameron@ryerson.ca.

NUMERICAL SIMULATION OF A FUEL NOZZLE'S
SPRAY

by

Ashley Ann Marie Fergusson

Bachelor of Engineering, Ryerson, 2009

A thesis

presented to Ryerson University

in partial fulfillment of the
requirements for the degree of
Master of Applied Science
in the Program of
Aerospace Engineering

Toronto, Ontario, Canada, 2011

©Ashley Ann Marie Fergusson 2011

I hereby declare that I am the sole author of this thesis.

I authorize Ryerson University to lend this thesis to other institutions or individuals for the purpose of scholarly research.

I further authorize Ryerson University to reproduce this thesis by photocopying or by other means, in total or in part, at the request of other institutions or individuals for the purpose of scholarly research.

Numerical Simulation of a Fuel Nozzle's Spray

Master of Applied Science 2011

Ashley Ann Marie Fergusson

Aerospace Engineering

Ryerson University

Abstract

The aim of this thesis is to examine the boundary conditions that must be input into the computational fluid dynamic software, FLUENT in order to model spray. This can then be used to advance the current computational fluid dynamic models used to model an engine's combustor. This will save the industry time and money, in the design and development stages.

The parameters that were studied in this thesis included, changing the angle the spray is injected at and the Rosin-Rammler parameters: number of droplet diameters contained within the spray and the droplet diameters spread, determining the uniformity of the spread.

The results found that it was possible to predict the Rosin-Rammler plot with a minor change of the Rosin-Rammler parameter, spread, q . It was also found that the initial assessments of the spray parameters provide reasonable trends in the axial and radial velocities.

Dedication

For my family and friends, who gave me unconditional support and love during this thesis. To Pratt and Whitney Canada and their staff, specifically my supervisor John Hu, and my colleagues Hang Xu and Dan Titirica for their much appreciated support and guidance. Finally, My Professors at Ryerson, Dr. Kamran Behdinan and Dr. Jeffrey Yokota for all their editing, encouragement and advice.

Contents

1	Introduction	1
1.1	Background	2
1.1.1	Fuel Spray	2
1.1.2	Combustor Modeling Benefits	3
1.1.3	Experimental Work	3
1.1.4	Numerical model	4
2	Sprays	7
2.1	Spray and Combustion	7
2.2	Fluid Dynamic Properties of a Spray	7
2.2.1	Mathematical modeling	8
2.3	Experimental Modeling	10
2.3.1	Phase Doppler Particle Analyzer (PDPA)	11
2.3.2	Patternators	11
2.4	Numerical Modeling	12
2.4.1	FLUENT Models	12
2.5	Drop Diameter Distribution	13
3	Nozzle Hardware	15
3.1	Simplex / Duplex	16
3.2	Pressure	17
3.3	Air-Assist	18
3.4	Air-Blast	18
3.5	Hybrid Fuel Nozzle	20
3.6	Nozzle Selection	20

4	Method	21
4.1	Geometry	21
4.2	Mesh Creation	22
4.3	FLUENT Injection Simulation Set-up	24
4.4	Injection Type	24
4.5	Injection Point Properties	26
4.6	Calc. for Fuel Inject. Initial Param.	27
4.6.1	Fuel Flow Rate	27
4.6.2	Droplet Velocity	27
4.7	Solution Methods	28
4.8	Assumptions	28
5	Results	29
5.1	Initial Setup and Test Case	29
5.2	Spray Addition	33
5.3	The Numerical Model and Study	34
5.3.1	The Variables	35
5.3.2	The Results of the Simulation	35
6	Conclusions and Future Work	69
6.1	Conclusions	69
6.2	Future Work	72
	References	79

List of Tables

2.1	Comparison of a Spring-Mass System to a Distorting Droplet [3]	12
5.1	Boundary Conditions	31

List of Figures

2.1	Spray Development[8]	8
2.2	PDPA Schematic [19]	11
3.1	Duplex Nozzle[8]	16
3.2	Flow Rate Vs. Injection Pressure of a Simplex and Duplex Nozzle [8] . .	17
3.3	Pressure Nozzle [8]	17
3.4	Air Assist Nozzle [8]	18
3.5	Air Blast Schematic [8]	19
3.6	Air Blast Nozzle and its components [8]	19
3.7	Hybrid Nozzle, Dotted Arrow-Air, Solid Arrow Fuel	20
4.1	Simplified Nozzle	22
4.2	Control Volume Cylinder	24
4.3	Control Volume Mesh	25
4.4	Nozzle Mesh	26
5.1	Basic Control Volume Cylinder	30
5.2	Control Volume Cylinder	30
5.3	Air Flow Velocity Magnitude Plot	32
5.4	Air Flow Dynamic Pressure Plot	32
5.5	Baseline Particle Tracking	34
5.6	Baseline Vs. PDPA	37
5.7	PDPA Vs. Modified Rosin-Rammler	38
5.8	Varying the Spread of the Diameters -Baseline Conditions	39
5.9	Varying the Spread of the Diameters (q) -Modified Baseline Condition . .	40
5.10	Varying the Sauter Mean Diameter – Baseline Condition	41

5.11 Varying the Sauter Mean Diameter-Modified Baseline Condition	42
5.12 Rosin-Rammler Plots - All Spray Variations	43
5.13 Mean Radial CFD Velocities Vs. the Radial Length of the Nozzle	46
5.14 Mean Axial CFD Velocities Vs. the Radial Length of the Nozzle	47
5.15 Mean Tangential CFD Velocities Vs. the Radial Length of the Nozzle	48
5.16 Mean Axial CFD Velocities Vs. the Radial Length of the Nozzle Vs the PDPA Results	49
5.17 Mean Radial CFD Velocities Vs. the Radial Length of the Nozzle Vs the PDPA Results	49
5.18 Unsymmertrical Mean Radial CFD Velocities Vs. the Radial Length of the Nozzle Plot- Baseline Parameter	50
5.19 Contours of Number of Particles - Baseline Condition	50
5.20 Contours of Number of Particles - Condition Reducing the in Initial Spray Angle By 10%	51
5.21 Contours of Number of Particles - Condition Increasing the Initial Spray Angle By 10%	51
5.22 Contours of Number of Particles - The Rosin-Rammler Number of Classes Parameter	52
5.23 Contour of DPM Number of Particles – The Rosin-Rammler Spread Pa- rameter	52
5.24 Air-Box cut away view	53
5.25 Air-Box Velocity Vectors	54
5.26 Air-Box Velocity Contours	54
5.27 Axial View of Nozzle - Velocity Magnitude Plot	55
5.28 Air-Box Pressure Contours	55
5.29 Contours of Concentration - Baseline Condition	57
5.30 Contours of Concentration - The Rosin-Rammler Spread Parameter	57
5.31 Contours of Concentration - Condition Increasing the Initial Spray Angle By 10%	58
5.32 Contours of Concentration - Condition Reducing the in Initial Spray Angle By 10%	58
5.33 Contours of Concentration - The Rosin-Rammler Number of Classes Pa- rameter	59

5.34	Patternation Annulus Collector Diagram	60
5.35	Percentage of Fuel Mass Vs. Radial Length Cross-Section 1	61
5.36	Percentage of Fuel Mass Vs. Radial Length Cross-Section 2	61
5.37	Percentage of Fuel Mass Vs. Radial Length Cross-Section 3	62
5.38	Percentage of Fuel Mass Vs. Radial Length Cross - Baseline Conditions .	62
5.39	Particle Traces Colored by Particle Diameter (m) - Baseline Condition .	63
5.40	Particle Traces Colored by Particle Mass (kg) - Baseline Condition	64
5.41	Particle Traces Colored by Particle Diameter (m)- Condition Reducing the in Initial Spray Angle By 10%	64
5.42	Particle Traces Colored by Particle Mass (kg)- Condition Reducing the in Initial Spray Angle By 10%	65
5.43	Particle Traces Colored by Particle Diameter (m)- Condition Increasing the Initial Spray Angle By 10%	65
5.44	Particle Traces Colored by Particle Mass (kg) - Condition Increasing the Initial Spray Angle By 10%	66
5.45	Particle Traces Colored by Particle Diameter (m) - The Rosin-Rammler Spread Parameter	66
5.46	Particle Traces Colored by Particle Mass (kg) - The Rosin-Rammler Spread Parameter	67
5.47	Particle Traces Colored by Particle Diameter (m) - The Rosin-Rammler Number of Classes Parameter	67
5.48	Particle Traces Colored by Particle Mass (kg) - The Rosin-Rammler Num- ber of Classes Parameter	68
A.1	Contours of DPM Concentration - Baseline Condition	74
A.2	Contours of DPM Concentration - Condition Reducing the in Initial Spray Angle By 10%	74
A.3	Contours of DPM Concentration - The Rosin-Rammler Number of Classes Parameter	75
A.4	Contours of DPM Concentration - Condition Increasing the Initial Spray Angle By 10%	75
A.5	Contours of DPM Concentration - The Rosin-Rammler Spread Parameter	76

List of Appendices

A Concentration Plots Created On a Plane 1.5 Inches From the Nozzle Face	73
---	----

List of Symbols

$P_{manifold} - P_{combustor}$ Change in Fuel Pressure across the nozzle

\bar{D} Arithmetic mean diameter of the two parcels

\bar{u} RMS value of the velocity fluctuations

λ_{opt} optimum wavelength

μ dynamic viscosity ($\frac{m^2}{s}$)

ν droplet velocity (m/s)

ru root-mean-square of the velocity fluctuations

ρ density of the fluid (kg/m^3)

ρ_A density of the air

ρ_f fuel density

ρ_L density of the Liquid

σ standard deviation, or surface tension, $\frac{kg}{s^2}$

C_D Drag coefficient of the drop

D droplet diameter, m

d The initial jet diameter

D_{max} Maximum Stable Droplet Size

FN	Nozzle Flow Number
l	characteristic length, taken as the droplet diameter (m)
Oh	Ohnesorge number
Q	the fraction of the total volume contained in drops of diameter less than D
q	the measure of the spread of the droplet sizes (infinity meaning a uniform droplet diameter spray)
Re	Reynolds number
$u_{average}$	Mean flow velocity
U_{rel}	relative velocity between two parcels
U_R	relative velocity between two parcels
V	Drop Velocity
We	Weber number
W_f	Fuel Flow Rate
We_{crit}	Weber critical condition

Chapter 1

Introduction

The impact a product has on the environment has become increasingly important to the aerospace industry in the preliminary design phase of jet engines [6]. The study of fuel injection characteristics within the jet engine can increase our understanding of combustion and therefore improve the efficiency of engines operation. Accurate computer modeling of the fuel injection spray into the engine can provide information about future soot and emissions to meet strict environmental requirements [24].

The engines combustion chamber is designed around the fuel injector's characteristics. The current process for estimating the fuel injector's characteristics in the aerospace industry is costly and time consuming, involving computer and mechanical testing. The process involves creating a model to study the individual aspect of a nozzle including their sprays distribution and the sprays breakup.

This study involves the use of a numerical model to simulate spray distribution. There are many characteristics of the spray that must be programmed into the numerical model to accurately create a realistic simulation. Many of these characteristics are unknown. This study will examine the relationship between the simulated spray characteristics and results obtained from experimental results. The results of this study will be useful for engineers to fine tune spray models.

This study demonstrates that each input parameter into the simulation has a unique and dramatic affect on the simulation's output and its correlation with the physical data. However, more importantly, it was the creation of a realistic simulation, incorporating all the complexities of spray injection, that would result in a good correlation with the

physical data.

1.1 Background

1.1.1 Fuel Spray

There is a great amount of interest in many industries for the creation of an accurate way to predict sprays. Some examples of this are, spray coating applications, and fire extinguishing sprays. High-quality spray coating needs a system that will deliver a constant performance [16] and a high impact velocity without the worry of overheating [17]. The Computational Fluid Dynamic, (CFD), code Fluent has been used to simulate the spray of a mist used to extinguish a pool-like gas fire. The result of this paper was that the simulated time to extinguishment was quite a bit longer than the measured laboratory data. More work on the modeling technique is needed possibly trying a droplet-vaporization model [1]. Work has been done on this subject in a report entitled, *A Dilute Spray Model for Fire Simulations: Formulation, Usage and Benchmark Problems*. This report uses a two-phase spray model to model dilute liquid or fire suppressant sprays. The simulation is modeled based on the stochastic separated flow, with the development and implementations of turbulence models for parcels and sub-parcel droplet dispersion, spray collision and spray breakup models. The results indicated that the approach was successful in providing an accurate and robust means to solve transport problems dealing with dispersed phase spray for fire applications [11].

Many papers have been written on the subject of spray modeling for engine applications. Papers have been written on the application of diesel engines. For example, the thesis *Development and Validation of Spray Models for Investigating Diesel Engine Combustion and Emissions* by Sibendu Som [24]. This paper discusses the increasingly stringent regulations on soot and NOx emissions of diesel engines. These engines are known for their high soot and NOx emissions. This paper recognizes the importance of the fuel injection characteristics and their effect on the combustion and the emissions processes, and improves on the primary breakup model. This model has been developed to incorporate cavitation, and turbulence effects as well as aerodynamically induced breakup. Many papers echo this idea that there is a lack of CFD codes that can accurately predict spray formation and the authors have made an efforts to improve the

simulation with the spray breakup model [9].

1.1.2 Combustor Modeling Benefits

The ability to accurately model the combustor presents many benefits to a designer. With the advent of biofuels, the ability to model different types of fuels allows the engineer to save experimental costs and gives them more freedom to try a variety of fuels, without the financial and hardware limitations that would exist if traditional mechanical methods were used. Rakopoulos et al [20], performed a study creating a two dimensional model to predict the emissions nitric oxide and soot formation. They implemented droplet evaporation and jet mixing models, and broke up their control volume into zones. A simulation was used to find the amount of fuel and entrained air in each zone, which was available for combustion. The concentrations of the species were calculated using the chemical equilibrium schemes and chemical rate equations. They found that the results compared well to those found on the test rig, proving the usefulness of this type of computational method [20].

1.1.3 Experimental Work

To validate the numerical modelings abilities to accurately simulate the spray, mechanical experimental data must be collected and compared to the numerical results. Early work has been performed by Sturgess et al. in 1985 entitled "Calculation of a hollow-cone liquid spray in a uniform airstream". This article discusses validating the numerical CFD code with mechanical data. The mechanical data was collected by using a double spark light source to take high-speed photographs of atomized drops of water in flight. The photographs allowed measurements of only the droplet size, velocity and angle of trajectory and did not allow for any temperature testing to occur [25].

The collection of mechanical data has improved greatly. One option that is used in this thesis is what is known as Phase-Doppler Particle Anemometry (PDPA). It is one of the most robust and reliable techniques for sizing spherical particles. [7]. The article by Qiu and Sommerfeld discusses "a reliable method for determining the measurement volume size and particle mass fluxes using phase-Doppler anemometry". This study compared the integration of the mass flux, which produces the mass flow rate in a water

spray with the global mass balance. The difference was found to be about 5% [14].

1.1.4 Numerical model

The paper entitled Issues Related to Spray Combustion Modeling Validation by M.G. Giridharan and al, provides some insight into why spray is so complicated to simulate and the issues that arise when these simulations are validated. The paper describes the database that was collected at the National Institute of Standards and Technology, which was a collection of benchmark spray combustion data and the validation data of a commercial CFD code. The preliminary results presented in the paper show a qualitative agreement between the CFD data and the measured data. The authors concluded that the major issue was specifying the initial conditions that accurately mirrored the laboratory conditions. This is exactly the aim of this thesis. [13]

One successful application of using the CFD software, FLUENT, was with gasoline direct injection engines. For example, the paper entitled "Spray Pattern Recognition for Multi-Hole Gasoline Direct Injectors using CFD Modeling" used the FLUENT code and the built-in TAB breakup model. The results were reported to vary slightly from the measured data. However, the results were still considered a good prediction of spray. [22]

Aerospace Companies have been actively researching numerical spray modeling techniques. One example is General Electric, who has been doing this kind of work for many years. The paper, "An Advanced Spray Model for Application to the Prediction of Gas Turbine Combustion Flow Fields", discusses the work of General Electric, and their evaluation of the advanced quasi-steady droplet vaporization model.

Thesis Objective and Strategy

Can a spray from a fuel nozzle be modelled accurately by the CFD software FLUENT?

The strategy that will be used is creating a FLUENT model using a given geometry and a cylindrical control volume. The FLUENT injection tool will be used to model spray injection into the control volume. The results will be compared to experimental data's Rosin-Rammler plots, Velocity data and patternation data.

My contribution to the industry will be to provide more information about the initial boundary conditions needed to create an accurate model of spray. This will then be used

to advance the current CFD models used to model and engine's combustor. This will save the industry time and money.

Thesis Layout

The layout of this thesis is as follows:

An introduction to spray, its fluid dynamic properties, experimental modeling techniques and numerical modeling abilities, Chapter 2.

An overview of nozzle hardware, the different parts and types of nozzles, Chapter 3.

Chapter 4 includes an overview of the methods used for the thesis.

Chapter 5 includes the results of the thesis.

Finally, Chapter 6 includes the conclusions and suggestions for future work.

Chapter 2

Sprays

2.1 Spray and Combustion

The performance of a gas turbine combustion system relies on effective liquid atomization and evaporation of the fuel. Normal liquid fuels are not adequately volatile to produce vapour in the volume necessary for ignition or combustion. The liquid must be atomized in to smaller droplets in order to increase the surface area of the droplets and to increase the rate of evaporation [8]. The preparation of the fuel within the combustor is very important to the engines performance, because a large increase in the ignition energy is necessity to counteract even a tiny increase in the mean drop size. The fuel injection also affects the stability limits, combustion efficiency and the emission pollution levels [8].

2.2 Fluid Dynamic Properties of a Spray

Figure 2.1, shows the progression of a spray with the increase in pressure. As the pressure increases the spray progresses from a dribble to an onion fuel sheet stage to a fine atomization.

A spray is defined as two-phase flow. The liquid being in the form of dispersed, or discrete phase droplets or ligaments, and gas in the continuous phase [23]. A stream of liquid breaks up into droplets because of internal and external forces acting on the surface tension. The stream will break up into droplets when the magnitude of the disruptive internal or external forces exceeds that of the surface tension [8]. If no forces act on a

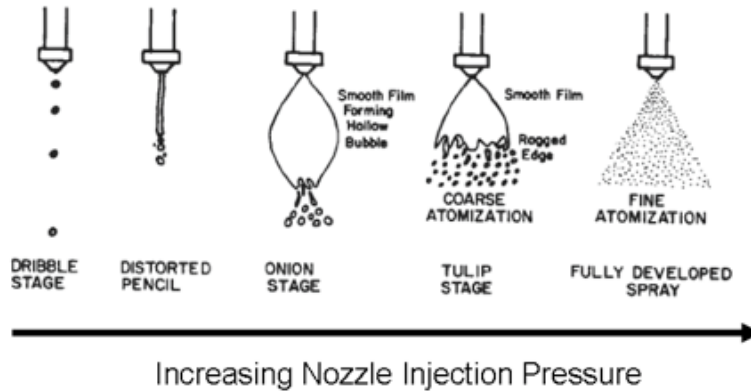


Figure 2.1: Spray Development[8]

droplet then the minimum surface energy is used and the droplet forms a sphere [8].

The break up of a stream of liquid, or otherwise known as atomization, happens in two stages. The primary atomization happens when the stream broken up into shreds and ligaments. The secondary atomization happens when these shreds and ligaments broken up into smaller droplets [8]. The nozzle does this by shearing the fuel against the air sheets that the nozzle produces. The frictional shear forces between these two liquids cause the fuel to break up [8].

2.2.1 Mathematical modeling

The Weber Number (We), is the ratio of aerodynamic forces to surface tension forces, described in Equation 2.1. The higher the number, the higher the deforming external pressures force [8].

$$We = \frac{\rho_L U_R^2 D}{\sigma} \quad (2.1)$$

The Weber critical condition is an important point at which the aerodynamic drag is equal to the surface tension force. This condition contains the largest droplets as it is broken up with the minimal amount of energy. This point is useful because it is a baseline that can be defined. This point is defined below in Equation 2.2 [8].

$$C_D \frac{\pi}{4} D^2 \frac{1}{2} \rho_A U_R^2 = \pi D \sigma \quad (2.2)$$

A useful application for this condition is when considering evaporation. The equations used for evaporation consider only the largest stable droplet in the spray for a relative velocity, U_R , Equation 2.3 [8].

$$D_{max} = \frac{12\sigma}{\rho_A U_R^2} \quad (2.3)$$

Based on experimental data, low-viscosity fuels can be estimated as in Equation 2.4.

$$W_{e_{crit}} = 12 \quad (2.4)$$

The Weber number can also help account for the influence of liquid viscosity on drop breakup with the Ohnesorge number, Oh , Equation 2.5. [8][15]

$$Oh = \frac{(W_e)^{0.5}}{Re} = \frac{\mu}{(\rho\sigma D)^{0.5}} \quad (2.5)$$

In 1967, Brodkey was able to find an expression that combined the Weber number, which is the expression for the aerodynamic forces, together with the viscosity influences described by the Ohnesorge number, in Equation 2.6[8][10].

$$W_{e_{crit}} = W_{e_{critZeroVelocity}} + 14Oh^{1.6} \quad (2.6)$$

The above equations assume a relatively high velocity between the fuel droplets and the surrounding air. This is not always the case as droplets become airborne shortly after leaving the nozzle. Therefore it is more logical to assume that the size of the droplets is determined by the dynamic pressure forces of the turbulent motion of the surrounding air-stream, Equation 2.7 [8].

$$W_{e_{crit}} = \frac{\rho_A \bar{u}^2 D_{max}}{\sigma} \quad (2.7)$$

According to Sevik and Park, [18]

$$W_{e_{crit}} = 1.04 \quad (2.8)$$

$$D_{max} = \frac{1.04\sigma}{\rho_A \bar{u}^2} \quad (2.9)$$

According to Rayleigh, the growth of small disturbances in the fuel sheet leads to breakup when the fastest growing disturbances hits an optimum wavelength, Equation 2.10. This produces a cylindrical drop of 4.51 times the initial jet diameter. This droplet then becomes a cylinder equaling 1.89 times the initial jet diameter [8][21].

$$\lambda_{opt} = 4.51d \quad (2.10)$$

Weber extended Rayleigh's work to include the viscosity effects shown in Equation 2.11 [26].

$$\lambda_{opt} = 4.44d(1 + 3Oh)^{0.5} \quad (2.11)$$

It was found that the effect of increasing the relative velocity between the fuel jet and the surrounding air reduced the optimum wavelength for the jet breakup, and therefore smaller droplet sizes are produced [8].

Fuel Sheets

Most atomizers discharge fuel in a hollow cone, or conical sheet. This is formed when fuel flows through tangential or helical slot with a tangential velocity component. A wave motion is generated because of a relative velocity between the fuel sheet and the surrounding air. This causes rings of fuel to break off from the leading edge with a width of the ring equal to one-half of the wavelength of the oscillation [8].

2.3 Experimental Modeling

It is near impossible to replicate the conditions within a combustor to test the fuel spray. The temperature and pressures within the combustor is too high to safely replicate, therefore a scaled down version of the spray is used. Two popular ways of experimentally characterizing sprays are Phase Doppler Particle Analyzer (PDPA) and using a Patternator.

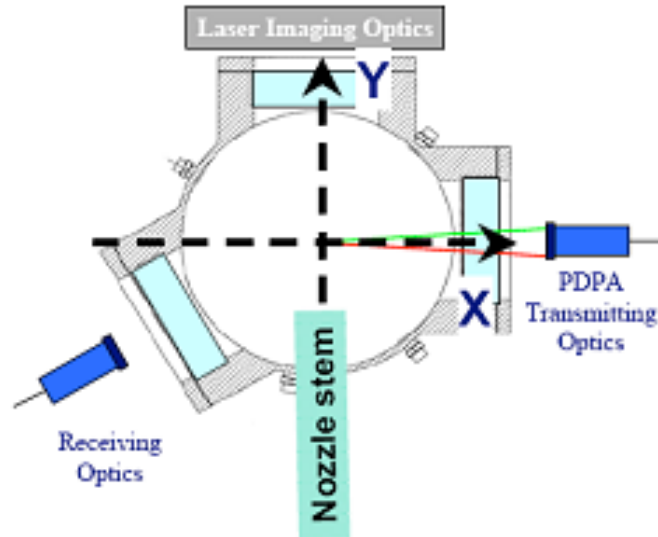


Figure 2.2: PDPA Schematic [19]

2.3.1 Phase Doppler Particle Analyzer (PDPA)

PDPA functions on the principles of light scattering interferometry. It is one of the most robust and reliable techniques for sizing spherical particles [7]. This method, shown in Figure 2.2 involves particles moving in the x-direction through a probe volume and scattering the incident light beams located in the x-y plane. Detectors located in the y-z plane then pick up the scattered light; these detectors collect the data in three different areas of the lens and by three separate photo detectors. The output from the detectors is a Doppler burst. The size of the moving droplets is the difference in phase between the detectors outputs [7].

2.3.2 Patternators

The Patternators main function is to determine the distribution of fuel dispersed from the nozzle and the location of where the fuel droplets are at a distance away from the face of the nozzle. Using the nozzle to flow air and spray fuel into the rig, the rig collects the fuel mass into multiple tubes. Measuring the amount of fuel within these tubes tells the engineer how the fuel is being distributed within the combustor. This test is popular because it is relatively low cost both fiscally and time-wise.

Spring-Mass System	Distorting and Oscillating Droplet
Restoring force of spring	Surface tension forces
External force	Droplet drag forces
Damping force	Droplet viscosity forces

Table 2.1: Comparison of a Spring-Mass System to a Distorting Droplet [3]

2.4 Numerical Modeling

2.4.1 FLUENT Models

To model a spray within the CFD software FLUENT there are two models that can be used to model the droplet break up and the collisions between the droplets.

Secondary Breakup Model Theory

The breakup model has two options, the Wave and the Taylor Analogy Breakup Model (TAB). The Wave model is used for high-Weber-number flows. This model is appropriate for high-speed injections. For this thesis, the TAB model is utilized because it is best used for low-Weber-number sprays where the Wave Breakup Model is best used for high-speed injections. The Weber number is defined in equation 2.12 [3].

$$W_e = \frac{\rho v^2 l}{\sigma} \quad (2.12)$$

On the fuel nozzle being studied here, the surface tension would be relatively high due to the low speed patternation and PDPA conditions. Since the test conditions are reduced for testing in these rigs the velocity would be relatively low. The TAB model considers an oscillating and distorting droplet to be like a spring mass system. This relationship is shown in Table 2.1[3][4].

Collision Model Theory

This model is used to evaluate the number of collisions there are between the droplets and the outcomes of the droplet collisions. To simplify the computation and limit the computational cost, the droplets are considered in parcels of droplets. Each parcel contains a certain number of droplets. This reduces the number of collisions that the computer

must calculate. The program uses O'Rourke's method to determine if two parcels would intersect. Once it is determined that they do, the computer then determines what type of collision occurs, either coalescence or bouncing. The probability of each is calculated using Equation 2.13 [3][4].

$$W_e = \frac{\rho U_{rel}^2 \bar{D}}{\sigma} \quad (2.13)$$

2.5 Drop Diameter Distribution

Rosin-Rammler

Rosin-Rammler distribution is an expression used to determine the droplet size distribution of a spray, equation 2.14, in terms of X and q [8].

$$1 - Q = e^{-(\frac{D}{\bar{X}})^q} \quad (2.14)$$

q , denotes the spread of the drop sizes, the higher the value the more uniform the spray. As q moves toward infinity the drops become of uniform size. The most practical sprays have q s that range 1.8 to 3.0. X denotes the droplet diameter [8]. This distribution assumes an infinite range of drop sizes and allows the data to be extrapolated into very fine droplets, an area which measurements are most difficult and least accurate [8].

Chapter 3

Nozzle Hardware

The main function of a fuel nozzle is to deliver fuel to the combustion area where it is ignited to add energy to the air. It is desirable for the air and fuel to be consumed within the combustor. The air and the fuel must mix for efficient combustion to occur. The jet engine fuel nozzle is broken up into two parts, the fuel nozzle and the atomizer. The fuel nozzle is where the fuel is injected into the combustor chamber. The atomizer is a passage or nozzle where air flows through, designed to breakup the fuel droplets. The air is generally swirling at high pressure to ensure good breakup or dispersion of the fuel droplets, the technical term for this action is atomization of the fuel droplets.

There are five major parts to a fuel nozzle: The inlet adapter, the flange, the stem, the heat shield or sheath and the tip assembly. The inlet adapter and the flange is to attach the nozzle to the combustor. The stem contains the major fuel passages between the inlet and the tip of the nozzle. The shield protects the stem from pressurized air and insulates the fuel passages. The tip defines the type of nozzle and it includes the atomizer.

The general requirements for an atomizer to be effective are as follows. First, the atomizer must be able to provide a uniform fuel distribution over a wide range of flow rates. Secondly, it must be able to respond to changes in fuel flow and be free of instabilities in the flow. Thirdly, It must be able to function blockage free, including preventing buildup of carbon on the nozzle face. Fourthly, it must not be susceptible to gum formation created by heat soakage. Finally, it must meet all the rest of the requirements of a good engineering design. For example, easy to repair, able to be scalable to allow for design

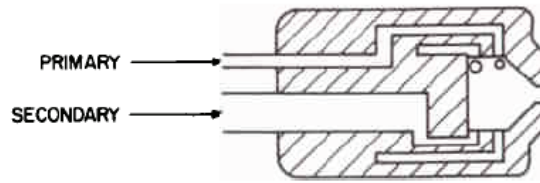


Figure 3.1: Duplex Nozzle[8]

flexibility, low cost, light weight and easy to remove for servicing.

There are many different fuel nozzle designs used for jet engine applications. The most common categories are the pressure, air-blast, air-assist, and hybrid models. It is also interesting to note that each company has their own way of defining each fuel nozzle air distribution. There are various applications for the different nozzles during the engines operation. At ignition, starter fuel nozzles have a wider cone angle ensuring the fuel is interacting efficiently with the igniter during cold-starts and the flight envelope. The specific nozzle design selection is based on the ignition source, fuel pump, the need for depleted battery starts, fuel control and the combustor.

In the design phase of a nozzle two types of analysis are performed: dynamic and thermal, stress and life analysis. The nozzle must also go through development testing which include tests like patternation, and tap tests, and substantiation testing which include emissions testing, altitude relights and smoke testing.

3.1 Simplex / Duplex

The first major categorization is how the fuel is delivered to the combustion chamber. The two categories of nozzles are simplex or duplex. The simplex nozzle provides only one spray, whereas the duplex nozzle, Figure 3.1 provides two sprays, which allows more control over how the spray is atomized. An example of this is shown in the Figure 3.2, where the flow rate of the simplex nozzle is consistent, whereas the duplex is not. The two sprays are known as the primary spray, the more concentrated spray used to start the engine, and the secondary spray, the hollow cone spray used when the engine is in a steady state or cruise.

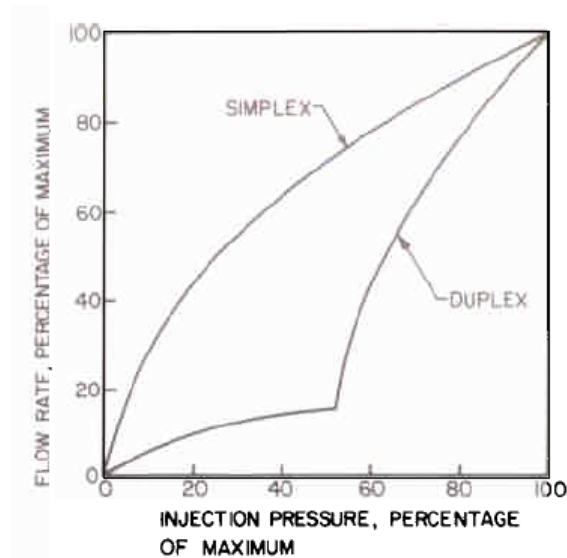


Figure 3.2: Flow Rate Vs. Injection Pressure of a Simplex and Duplex Nozzle [8]

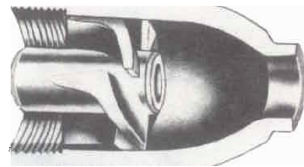


Figure 3.3: Pressure Nozzle [8]

3.2 Pressure

The pressure nozzle differs from the rest of the nozzles described below because it relies on fuel pressure to atomize the fuel. The pressure nozzle converts pressure, into kinetic energy to attain a high relative velocity between the fuel and the surrounding air. As can be seen in Figure 3.3, the nozzle contains fins that swirl the fuel in order to improve the atomization of the fuel. This nozzle can be used in simplex nozzles and duplex injectors[8].

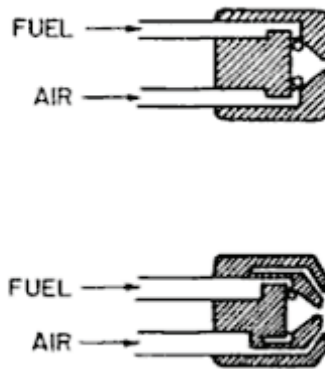


Figure 3.4: Air Assist Nozzle [8]

3.3 Air-Assist

The air-assist nozzle, Figure 3.4 relies on air to atomize the fuel. This means that the fuel which exits the nozzle in the form of a sheet is broken up by the shear force of the air. This shearing force is placed at an angle to the fuel sheet and breaks the sheets into droplets. An air-assist nozzle is a duplex nozzle meaning it is a pressure atomizer with an air-swirler attached to the fuels tip to improve the atomization. It is defined this way because the fuel is exposed to the air stream flowing at a high velocity, which is used to help atomize the fuel. This method tends to be inefficient, however it is able to create finer sprays than the pressure atomizer. There are two types of these nozzles: internal, which the air and fuel mix inside the nozzle and external, where the fuel and air mix outside the nozzle [8].

3.4 Air-Blast

Air-blast nozzle shown in Figure 3.5, is similar to the air-assist nozzle, however the air-blast nozzle provides a larger amount of air and lower pressures [8].

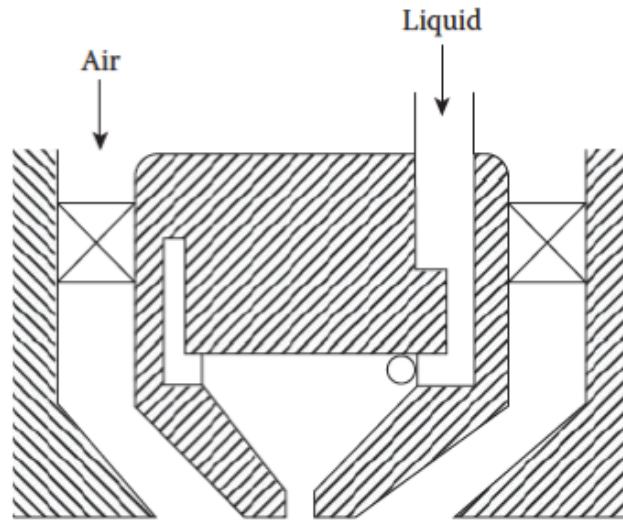


Figure 3.5: Air Blast Schematic [8]

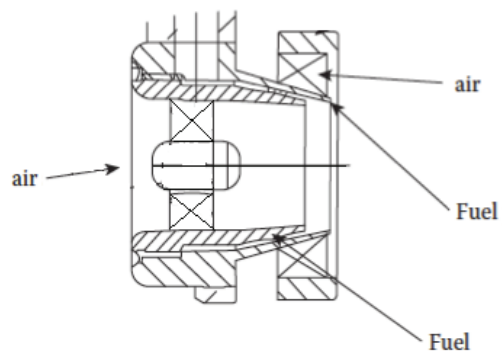


Figure 3.6: Air Blast Nozzle and its components [8]

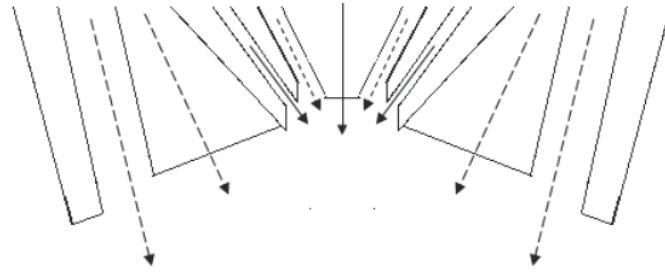


Figure 3.7: Hybrid Nozzle, Dotted Arrow-Air, Solid Arrow Fuel

3.5 Hybrid Fuel Nozzle

The hybrid nozzle is a combination of the above nozzles, shown in Figure 3.7. The hybrid nozzle is a duplex nozzle. It has an air-assist type nozzle configuration at its core. This means that the centre of the nozzle is a pressure fuel nozzle. This is surrounded by an air-assist type air nozzle and this is followed by the secondary fuel nozzle, which is then surrounded by an air-blast air nozzle and swirler.

3.6 Nozzle Selection

The nozzle model that was chosen for this thesis was based on the following criteria. The design of the nozzle had to have a complete solid cad model associated to it. The nozzle had to have all necessary up to date data so that it could be easily modelled. These criteria lead to the selection of a specific nozzle model. The model used was not selected based on ease of modeling and therefore this thesis is the modeling of spray of a specific nozzle design. However, the modeling methodology presented in this thesis could be used towards modeling other types of nozzles.

Chapter 4

Method

4.1 Geometry

The nozzle selected for this thesis is an air-assist nozzle. To begin this study, a 3-dimensional CAD model of the nozzle and the air-box was attained. An air-box is a box created for physical testing of the nozzle, which flows the air into the nozzle. It is a basic box that surrounds the inlet of the nozzle with air. These two models, the nozzle and the air-box, were joined in the appropriate configuration. The nozzle that was attained was what is known as an air solid. This means that it does not include any of the fuel passages, which is useful in this case as the fuel will be modelled as an injection from the normal injection location on the face of the nozzle. The air passages or what can be seen as the negative of the nozzle must be extracted in order for a fluid dynamic model to be created. This process was done by extracting all the surfaces that interact with the air flowing through the nozzle using the CATIA design software. These surfaces were then joined together. The areas of the nozzle that let air in or out were then capped to close the surface volume. A solid closed surface geometry was then created and ready for meshing.

Once meshing, it was found that the nozzle contained areas that were too small to accommodate the smallest elements allowed by the meshing program. These areas then had to be eliminated. It was found that one of these areas dealt with how the nozzle exit was capped. This area was the outside ring of the atomizer and this area was found to have small discontinuities that caused the area to not be perfectly round or flat. This

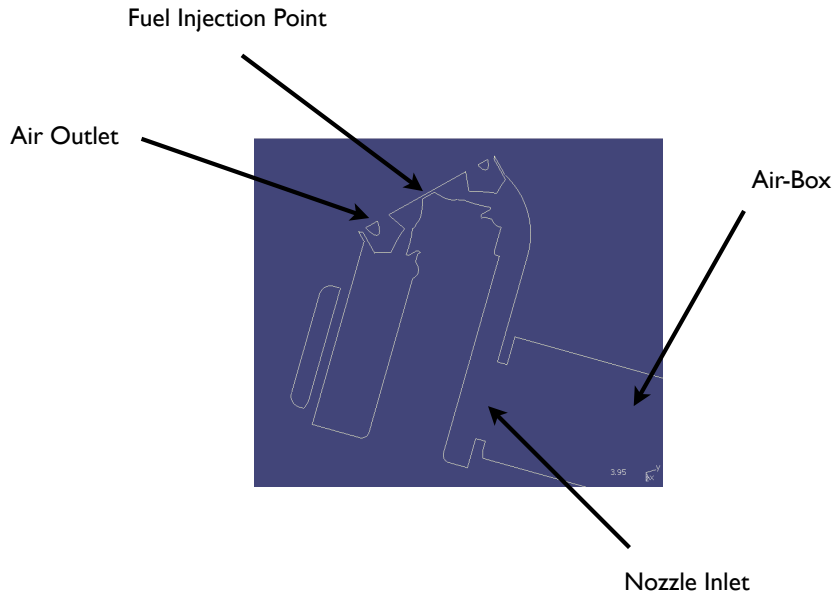


Figure 4.1: Simplified Nozzle

first had to be repaired. They were added to the design to so that the nozzle could fit into the combustor and so were not needed for this simulation. This meant that depending on which surface was chosen drastically affected the meshability of the part. Therefore, a position was found which maximized the area covered and decreased the amount of narrow areas.

4.2 Mesh Creation

To perform a CFD analysis a mesh must be created. This mesh must meet certain criteria in order to be successfully accepted by the CFD program. The driving parameter for FLUENT is the maximum cell skewness. The skewness must be below 0.98. This was the driving consideration when the mesh was created [2].

There are three main types of meshing techniques: Tetra, Prism and Hexa. Tetra meshing uses tetrahedral elements. This technique is useful for complex geometries because the element shape lends it self well to complex curves in the geometry. Prism

meshing is able to maintain the ease and the automation of Tetra meshing. However, it is able to better capture the shear or boundary layer physics. Hexa meshing is the semi-automatic option where as the rest are fully automatic. This method allows for more manual control of the mesh. This mesh uses hexahedral mesh elements [5].

The first meshing attempt was made using the Hexa technique. This technique was found to be hard to use and the cell skewness and quality required was not attainable. Therefore, for this mesh the Tetra technique was used.

Starting out, the mesh was created to optimize the number of elements that would be used to decrease the effort of the simulation software. The original geometry contained very thin parts; these parts were so thin that the width of the elements was too big to fit the geometry. This meant that these parts had to be removed because the software was not able to produce elements small enough to fit in these very thin components. Due to the complex nature of the nozzle, the elements that were used still had to be as small as possible in order to achieve the 0.98 skewness requirement. Therefore only one mesh, the finest possible with the computational abilities provided could be used for this application.

The control volume beneath the nozzle, Figure 5.2, had more options with regard to mesh density. The governing parameter for this section was the injection spray that would be caught by this control volume. The injection spray would not be evaluated with a course mesh. The mesh had to be changed and a trial and error technique was used to determine its mesh density. When the mesh was too course no results for the spray would be displayed.

The model was originally produced in two parts: part 1 being the nozzle and part 2 the control volume. This made the mesh easier to create as the nozzle could be given a finer mesh than the cylinder. When this mesh was imported in to FLUENT there was errors reported that could not be solved by small modifications to the mesh. Therefore, the geometry was modified to join the nozzle and the cylinder into one part. This eliminated any interfaces in the grid. This new geometry was then meshed and reintroduced into FLUENT.

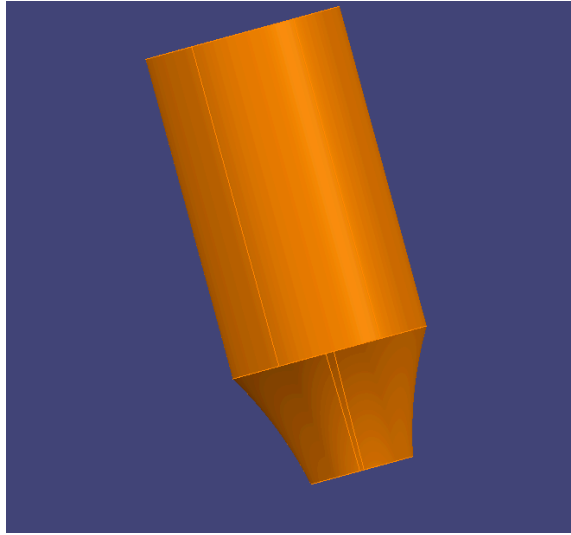


Figure 4.2: Control Volume Cylinder

4.3 FLUENT Injection Simulation Set-up

To set-up a FLUENT injection within the program, the injection properties must be established. This includes setting the particle type, material, injection type, point properties, and diameter distribution. The inert particle type was assumed because no evaporation was assumed to take place at low temperatures and when the spray is measured one inch from the nozzle face. The material was set to kerosene, which is a good representation of Jet-A fuel, and the specifications of this fuel were set automatically by FLUENT in the materials section.

4.4 Injection Type

For the injection type, the user can choose from a variety of models that include hollow cone, solid cone, single, group or even more complex plain-orifice-atomizer and pressure-swirl-atomizer type injections [12]. In this thesis, a solid cone was used for the primary fuel injection and a hollow cone was used for the secondary fuel injection. After examination of the primary fuel nozzle drawing the injection point was found to provide the fuel in a random manner fitting the definition of a solid cone spray. The secondary fuel

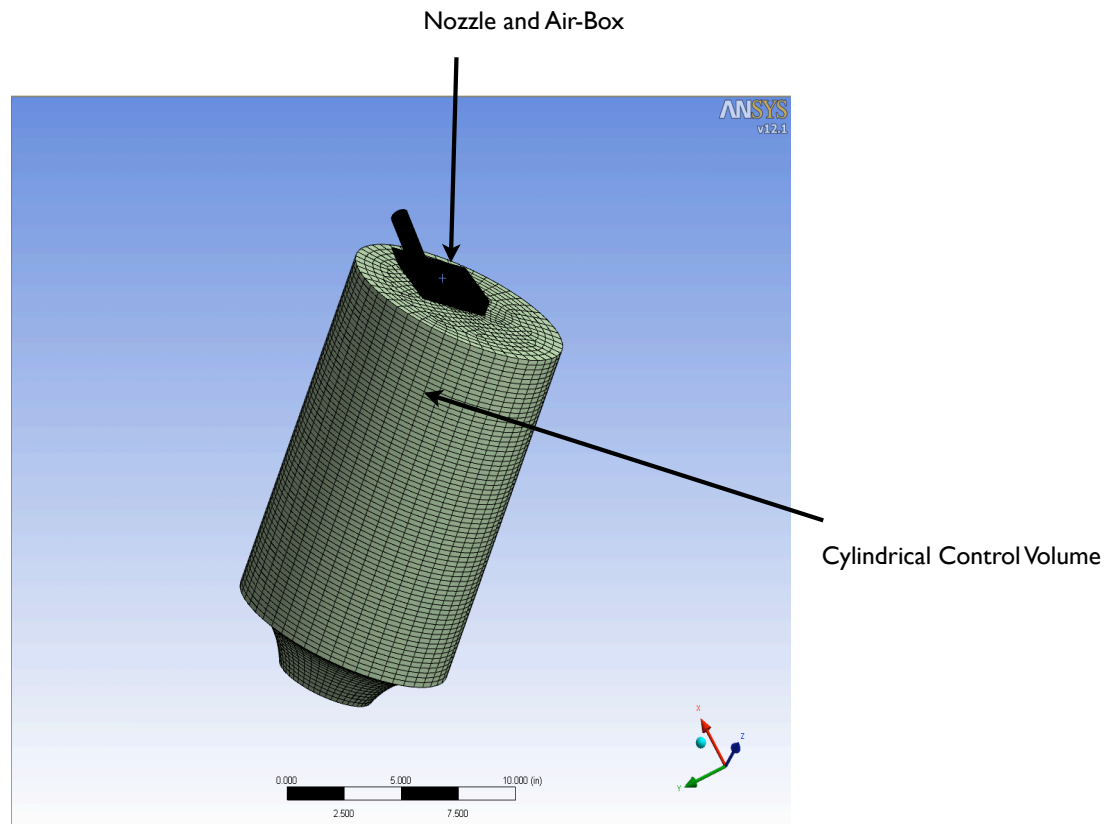


Figure 4.3: Control Volume Mesh

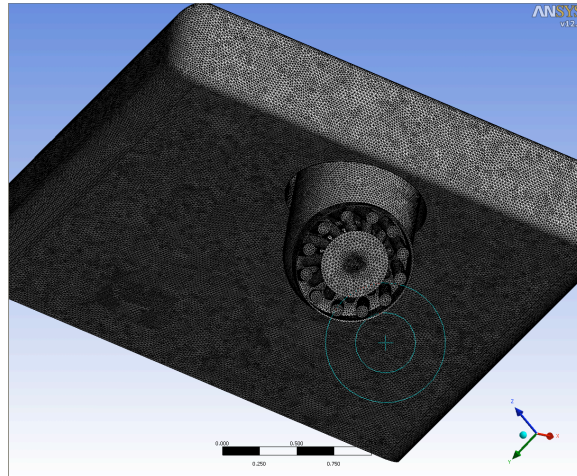


Figure 4.4: Nozzle Mesh

spray was modelled as a hollow cone due to the drawings specifications. [12]

4.5 Injection Point Properties

The first required point property is the X,Y,Z position. These positions were taken off the CATIA model. There was some concern about where these points should be taken. The first attempt was to put the point directly on the geometry wall. This proved to be unsuccessful, as it produced no results within the FLUENT simulation. The next attempt was to put the point just off the wall within the cylindrical calculation area. This proved successful. However, there was concern as to whether this would impact the results. The point should be placed behind the nozzle wall as the spray should be at the necessary angle when it exits the nozzle. The nozzle fuel passages were not included within the geometry, which was done for the simplification of meshing purposes. So, placing this point behind the nozzle wall was not possible as it would have to be placed within a nozzle passage that was not modelled. Instead the secondary spray was placed as close to the nozzle face as possible to address the concern of the difference of nozzle angles. This ensures that when the secondary nozzle passed the location of the primary nozzle, it was at the appropriate angle as to not interfere with the primary fuel spray.

4.6 Calculations for Fuel Injection Initial Parameters

4.6.1 Fuel Flow Rate

The fuel flow rate was calculated from the following equations found on the technical drawing. The first step was to find the flow number.

$$FN = \frac{W_f}{\sqrt{P_{manifold} - P_{combustor}}} \quad (4.1)$$

The present simulation uses 13 and 37 pounds per hour of primary and secondary fuel flow rates, respectively.

This allows for the fuel flow rates to be calculated using the same above equations and the appropriate fuel pressure ($P_{manifold} - P_{combustor}$) for the simulation being tested.

$$W_f = FN \sqrt{P_{manifold} - P_{combustor}} \quad (4.2)$$

4.6.2 Droplet Velocity

The droplet velocity was calculated using Equation 4.3 where the change in pressure ($P_{manifold} - P_{combustor}$) is the same as what was used above, and the density is the density of Jet-A fuel. This is acceptable as kerosene is very close in density to jet A fuel and makes a negligible change in the velocity. It is assumed that all the droplets in both the primary and secondary sprays will be injected at the same velocity.

$$V = \sqrt{\frac{P_{manifold} - P_{combustor}}{\rho_f}} \quad (4.3)$$

After some initial conditions were run and the experimental data examined, it was found that it was hard to distinguish how much fuel was injected from each of the primary and secondary fuel sources. The angle of the spray depended on the pressure applied on it. Therefore, it was difficult to determine the exact angle of the spray. For the final results an average of the fuel parameters were taken.

4.7 Solution Methods

The core equations or methods used within the simulation was the Standard Pressure, Green-Gauss Node Based Gradient method. The Coupled Scheme was used because velocity and pressure is strongly coupled. To ease the computation the First Order Upwind methods were used. This was because of the computational capabilities of the equipment used.

4.8 Assumptions

FLUENT has many advantages as there are many different options that one can take advantage of. This fact however can cause many unknowns and forces one to make some assumptions, for example when considering wall interactions. The Discrete Phase Reflection Coefficients were set to have the normal-constant parameter set to 0.1, causing a droplet that hits the wall to deform. The resulting deformed droplet velocity coming off the wall will be a tenth of the original. The tangent constant was set to 1 holding the tangential velocity constant.

The following assumptions were made in the boundary conditions. In reference to the turbulence boundary conditions, the Intensity and Length Scale Specification Method was selected based on known ease to define. The turbulent intensity can be found using Equation 4.4, however since the root-mean-square of the velocity fluctuations was unknown, the velocity intensity must be assumed. The Length scale was calculated using Equation 4.5.

$$TurbulentIntensity = \frac{Iu}{u_{average}} = 0.16Re_{DM}^{-\frac{1}{8}} \quad (4.4)$$

$$LengthScale = 0.07 * NozzleDiameter \quad (4.5)$$

Further assumptions must be made within the Rosin-Rammler Equation. The FLUENT model requires input of the minimum, the maximum and the mean droplet diameters. FLUENT also requires the spread parameter, which is the range of droplet diameters, and the number of droplet diameters needed within the spray. These values are all unknown and will be varied within the FLUENT simulation.

Chapter 5

Results

5.1 Initial Setup and Test Case

The first step in setting up a simulation is to ensure the mesh works, meaning that the mesh is at a quality that the CFD software can use. This is done by inputting the mesh into the FLUENT software and running the mesh check. The mesh check will run several checks on the mesh including one to ensure that the mesh meets the minimum cell skewness limit. This limit was of concern when creating the mesh for this study because the narrow passages in the complex geometry of the nozzle skewed the cells of the mesh.

To ensure the initial set-up of the simulation within FLUENT was correct, air was simulated to be passed through the mesh. This is the simplest case possible for this mesh and therefore included the least amount of possible places for errors.

The simplest simulation that can be run is a simple airflow through the bottom cylindrical control volume. Therefore, the nozzle mesh was unselected so that only the bottom cylindrical control volume remained active. This control volume is a basic cylinder with the inlet at the top of the cylinder and the outlet at the bottom of the cylinder shown in Figure 5.1. After iterating this simulation it was found that the solution did not easily converge. It was found that there was a great amount of air re-entering the control volume at the bottom of the cylinder known as reverse flow. To fix this problem, a cone was added to the bottom of the cylinder as shown in Figure 5.2. This reduced the size of the outlet of the mesh, increasing the pressure the air was exiting with and decreasing the chance of air entering the bottom of the cylinder. After this change was made, the

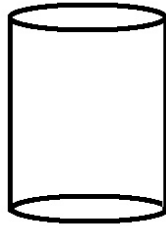


Figure 5.1: Basic Control Volume Cylinder

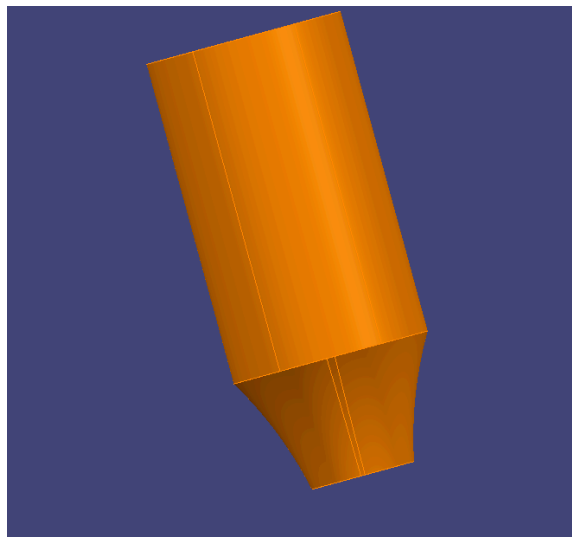


Figure 5.2: Control Volume Cylinder

simulation converged as expected.

The nozzle mesh was then reactivated so that both the nozzle mesh and the cylindrical mesh would be active in the simulation. After this mesh was input into FLUENT, FLUENT rejected the mesh. Many errors were present and the mesh check failed. To solve this problem the geometry was re-evaluated. The geometry was combined to include both the nozzle and the cylindrical control volume. This new geometry was re-meshed and input into FLUENT. The mesh was checked within FLUENT using its tool and the mesh passed.

The simulation that was run at it's simplest form passing only air through the mesh had the boundary conditions as are shown in Table 5.1.

Mass-Flow Inlet			
	Air Mass Flow rate	0.005709	kg/s
Outflow Outlet			
	Flow Rate Weighting	1	

Table 5.1: Boundary Conditions

The Mass flow inlet was chosen because it was found to provide a converged solution more easily than a pressure inlet.

The inlet air pressure and mass flow rate was received from experimental data and the outlet was defined as an outflow with a weighting of 1. The outlet boundary condition is set to this condition because the details of the flow velocity and the pressure are unknown. This boundary condition will allow FLUENT to extrapolate the required information from the interior. This boundary condition can be used in this case because this boundary is a single outflow rather than a split outflow meaning the flow rate weighting is set to 1. This boundary condition is also useable because the inlet boundary condition is a mass flow inlet and since the cylindrical control volume is so large, it is safe to assume the flow will be fully developed once it reaches this point.

As can be seen in Figures 5.3 and 5.4, the velocities and the pressure plots are realistic in that the air is flowing through the air-box and increasing in magnitude as the nozzle narrows. The magnitudes are also greater closer to the nozzle within the cylindrical control volume and decrease as it moves away from the nozzle face. The magnitudes of the velocity and the nozzle are as what is expected.

It was found that the point of reference for setting the initial pressure was found to be incorrect as well. To set the initial pressure of the control volume an X, Y, Z coordinate point must be set and an initial pressure value must be given to that point. This point must be set to the location within the control volume.

When these issues were corrected, the solution converged as expected meaning the simulation was ready to progress to the next stage of complexity by adding the fuel spray injection.

A solution is defined as converged when the changes in solution variables are negligible from one iteration to the next being smaller than 3 orders of magnitude to at least 10^{-3} . One should also check the mass balances. At a minimum the net mass imbalance should

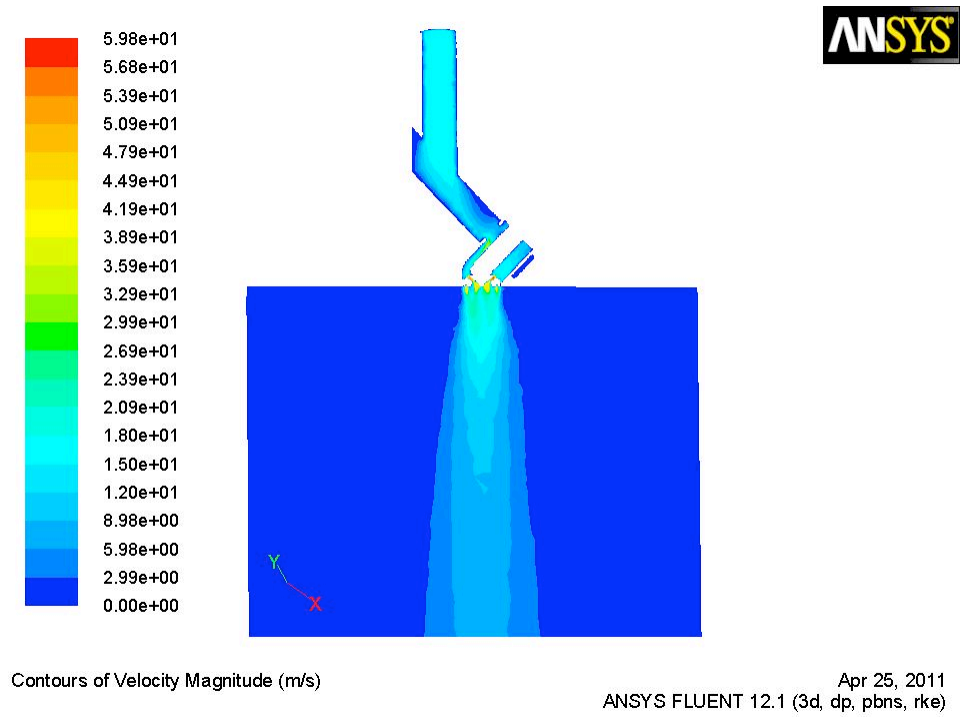


Figure 5.3: Air Flow Velocity Magnitude Plot

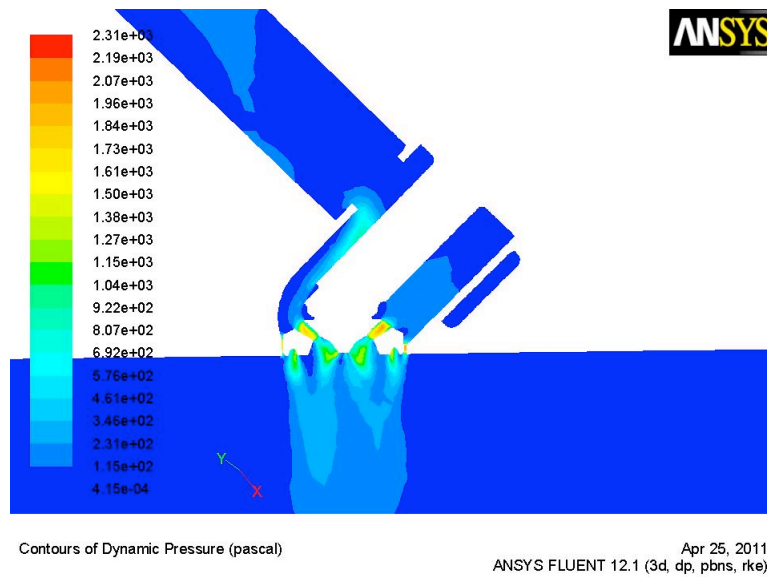


Figure 5.4: Air Flow Dynamic Pressure Plot

be less than 1% of the smallest flux through the domain [2].

5.2 Spray Addition

The next stage in the increasing complexity of this simulation is adding the fuel spray, which is injected by the fuel nozzle. This is a complex portion of this simulation because it involves ensuring many parameters are set correctly. The large number of parameters involved means there are a great number of possible errors that could occur. This is why this is the last part to be added to the simulation.

The number of injections to be added to this simulation was of constant debate. The injection types that were taken into consideration were the hollow cone and the solid cone. The hollow cone was modelled by FLUENT to be injected into the control volume initially as a fuel sheet and broken up by the air. This fuel sheet was defined with one initial radius. This implied that the thickness of this sheet was not known or defined. This meant that as more injection sources were added beside each other the droplets from each of the individual injection source began to interact. This caused FLUENT to delete some of the drops and drastically increased the time to converge a solution. Air was added flowing from the top surface of the control volume cylinder at 1 m/s. This helped wash the particles down the cylinder and fixed the aforementioned problems.

Another possible explanation to this error was that the spray angle was too large and the spray was leaving the cylindrical control volume. When the results were examined it was seen that the spray was well inside the control volume initially. However, when the spray interacted with the control volume wall it caused an error. This interaction was interesting because the boundary conditions put on the control volume wall was such that the particles were to reflect off. It was determined that since this interaction occurred well below the area of interest, the second line from the top on the cylindrical control volume in Figure 5.5 and the number of droplets that were being deleted were very small compared to the number of droplets in the system. It had little effect on the results extracted from the simulation. The initial number of injection sources were 20, 10 using the primary flow initial conditions and 10 using the secondary flow initial conditions.

After some investigation into experimental rig results, it was found that the percentage of the primary and the secondary spray in each area of the combustor was very similar.

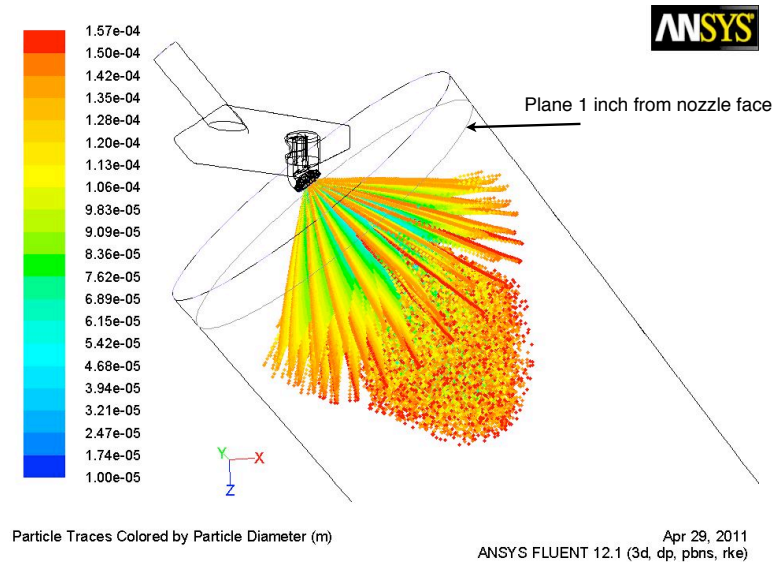


Figure 5.5: Baseline Particle Tracking

This meant that it was very hard to predict the individual initial injection conditions for each of these flows. Therefore, it was determined that the average of the flows would be injected, and 4 sources would be used to ease the computation.

5.3 The Numerical Model and The Study of It's Characteristics

A numerical model was produced to simulate spray distribution. The results of this model were compared to experimental data. A parametric study was performed on the model variables described below, to identify the sensitivities of the variables on the sprays characteristics, for example the velocity of the droplets and the distribution of the fuel concentration. This study will be useful for engineers to tune the spray model to match the measured data from the patternation and Phase Doppler Particle Analysis (PDPA). This will simplify the procedure used to model spray and make it more practical to use.

5.3.1 The Variables

Variables were developed based on unique parameters needed to setup the injections within the FLUENT program. The first simulation was run using baseline parameters. This case included a maximum, mean and minimum drop size of 174, 69 and 10 microns respectively. The Rosin-Rammler spread parameter was 3.41 and the number of droplet diameters contained within the spray, known as diameter classes, was set to 40. The angles of the 4 injections was set to 58, 83, 102, and 120 degrees respectively.

Varying the Rosin-Rammler Parameter Number of Classes

The first case varied the number of droplet diameters that are contained within the spray, also known as number of diameter classes. The spray breakup is a process that produces random results. It was hard to predict what the specific size of the droplets were in certain areas of the control volume. Therefore, this study varied the number of different droplet diameters that are present within the spray.

Varying the Spray Angle

The second and third simulations varied the spray angle. The pressure placed on the fuel dictates the angle in which the spray exits the nozzle. Therefore, it is unknown exactly what the spray angle is exiting the fuel nozzle because the nozzle in question is an air-assist nozzle, and therefore has a very complex geometry. This study examined the effect of increasing and decreasing the spray angle by 10 percent.

Varying the Spread of the Diameters

Lastly, the spread of the drop diameters was varied. This determines how uniform the spray was, the higher the value the more uniform the spray.

5.3.2 The Results of the Simulation

The general way that spray is analyzed is with volume flux, which is the rate of volume flow across a unit area. To find this value the mass flow rate must be found. The FLUENT software only provides this information at the boundary conditions of the mesh. The measurements of interest to this study are on a plane one inch from the nozzle face,

not on a boundary condition. Therefore, the volume flux cannot be obtained. However, there is a significant amount of data that is provided for this plane that can be compared to the PDPA. A comparison between the simulation results and the PDPA data is shown below.

Rosin-Rammler Plots

The Rosin-Rammler plot shows the percentage of drops that are of a certain size. This is a useful first step in evaluating a spray and how well the atomization process is working. The first step in plotting this graph is finding the \bar{X} and q for the spray. An explanation of these parameters are in Section 2.5. After examination of the PDPA data it was found that these parameters were calculated for each droplet in the control volume. Therefore, in order to plot the graph the values needed to be averaged in order to get one value for the spray. The CFD data was post processed in a similar fashion. This method however, left some room for interpretation as there was a spread between the Sauter Mean Diameter (SMD) used to calculate the \bar{X} and the q . Therefore, to determine the effects these values had on the Rosin-Rammler plots the maximum and minimum values found in the PDPA data was used to plot different Rosin-Rammler graphs using the baseline CFD condition. The results of this study are shown in Figures 5.8, and 5.10. Setting the SMD to 12 μm proved to reduce the drop diameters contained in the spray to a maximum of 20 μm . Increasing the SMD to 54 μm proved to increase the maximum drop diameter to 200 μm and increase the number of drops with larger diameters as well. Increasing the SMD to the PDPA's largest value of 95 μm proved increase the rate at which the drop size increased and reduced the amount of the smallest diameters. Varying the spread, q of the baseline condition had less of an effect to the profile of the graph than varying the SMD. Varying the q proved to alter the rate at which the drop size increased rather than affecting the values of the minimum and maximum of the drop diameters.

The variables discussed above proved to vary only with the number of diameter classes used and with varying the spread of the diameters used. Increasing or decreasing the spray angle proved to not alter the Rosin-Rammler plot from the baseline values.

To validate the simulation results, the baseline values were first plotted against the PDPA data shown in Figure 5.6. The baseline results compared well to the profile of

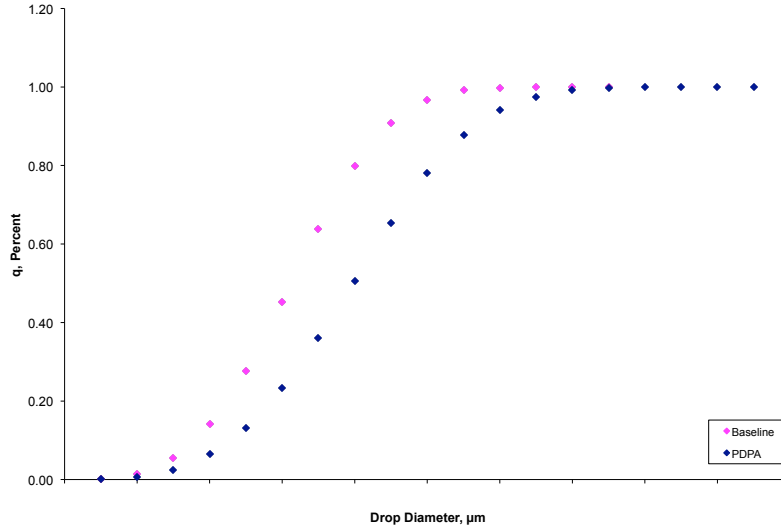


Figure 5.6: Baseline Vs. PDPA

the PDPA data. However, the baseline results were offset. According to Lefebvre, the Modified Rosin-Rammler expression has been shown to better represent some sets of data.[8] Also, the FLUENT software allows for the modified Rosin-Rammler distribution to be used during simulation. Therefore, another simulation was run changing the droplet distribution model to the Rosin-Rammler-logarithmic option. After post processing, it was found that using this distribution expression had little impact on the final results. However, a slight improvement was seen when using the modified distribution was plotted against the PDPA data using the modified Rosin-Rammler expression, Equation 5.1. This data had a smaller delta offset from the PDPA data and it followed the trend of the data fairly well with an average delta of 0.07.

$$1 - Q = e^{\left(\frac{\ln D}{\ln X}\right)^q} \quad (5.1)$$

Figure 5.8 shows that to match the profile of the PDPA data, a large spread must

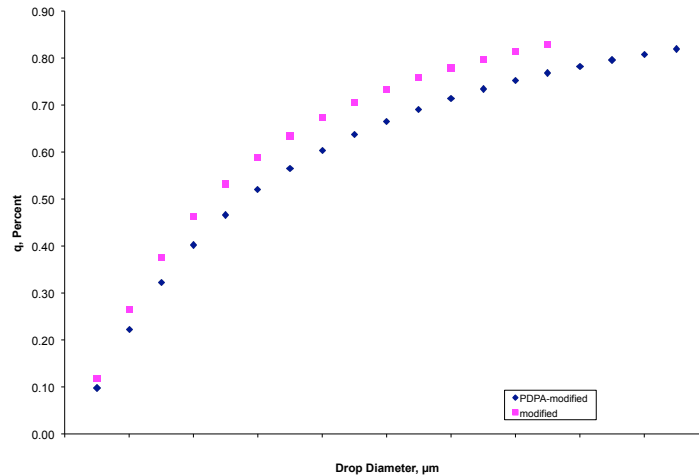


Figure 5.7: PDPA Vs. Modified Rosin-Rammler

be used for the smallest droplet diameters and the spread must decrease as the drop diameter increases, for the original Rosin-Rammler expression.

The opposite of this relation is true for the modified Rosin-Rammler distribution, the larger spread values seem to represent the smaller drop diameters better and the small spread values seem to follow the larger diameter values of the PDPA data, Figure 5.9.

Changing the SMD of the spray makes a larger difference as can be seen in Figure 5.10 and Figure 5.11. Changing the SMD has a greater affect on the profile of the points. This makes sense as a small SMD would mean that the mean drop diameter in that spray is less than that of a larger SMD. Therefore, the spray with the smaller SMD would represent a smaller amount of spray diameters as is the case of the SMD of 12 μm .

Changing the SMD on the modified plot provided subtler changes, as shown in Figure 5.11. The SMD of 12 μm was used, which represented less drop diameters than the rest making sense as the above explanation still applies. However the SMD of 95 and 54 both follow the profile of the PDPA data at an offset.

Simulations were also completed varying the variables in question, as shown in Figure

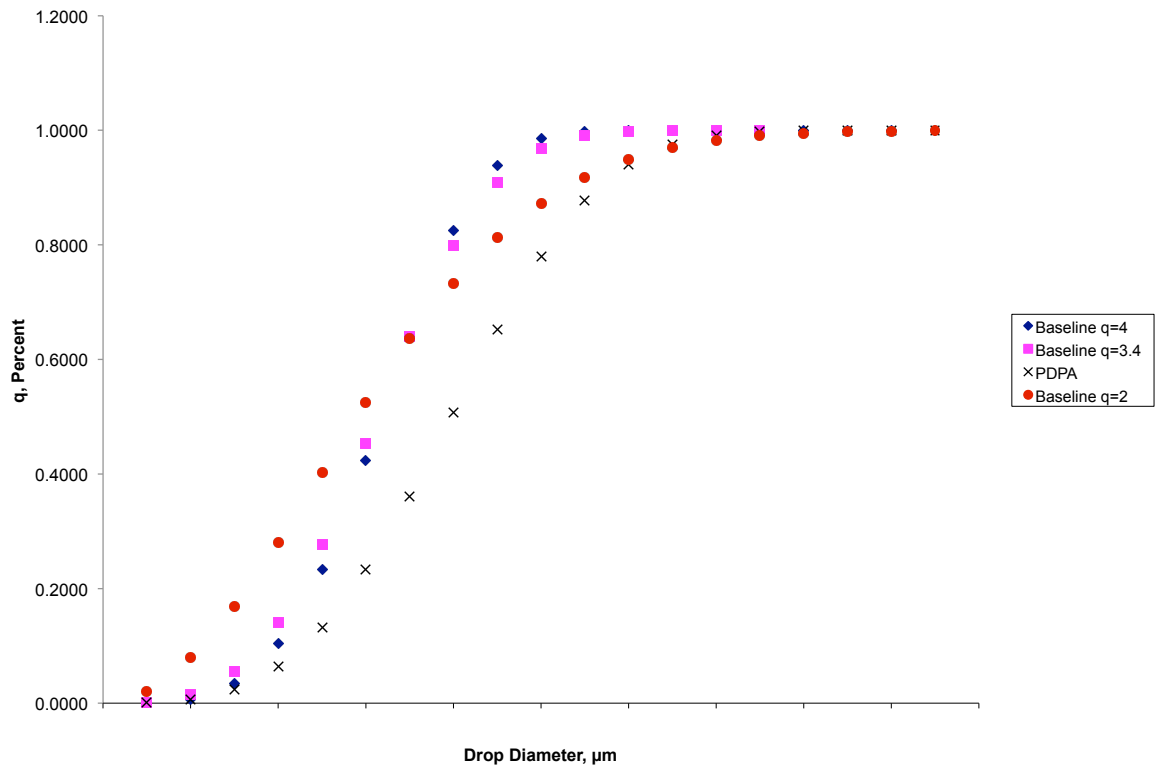
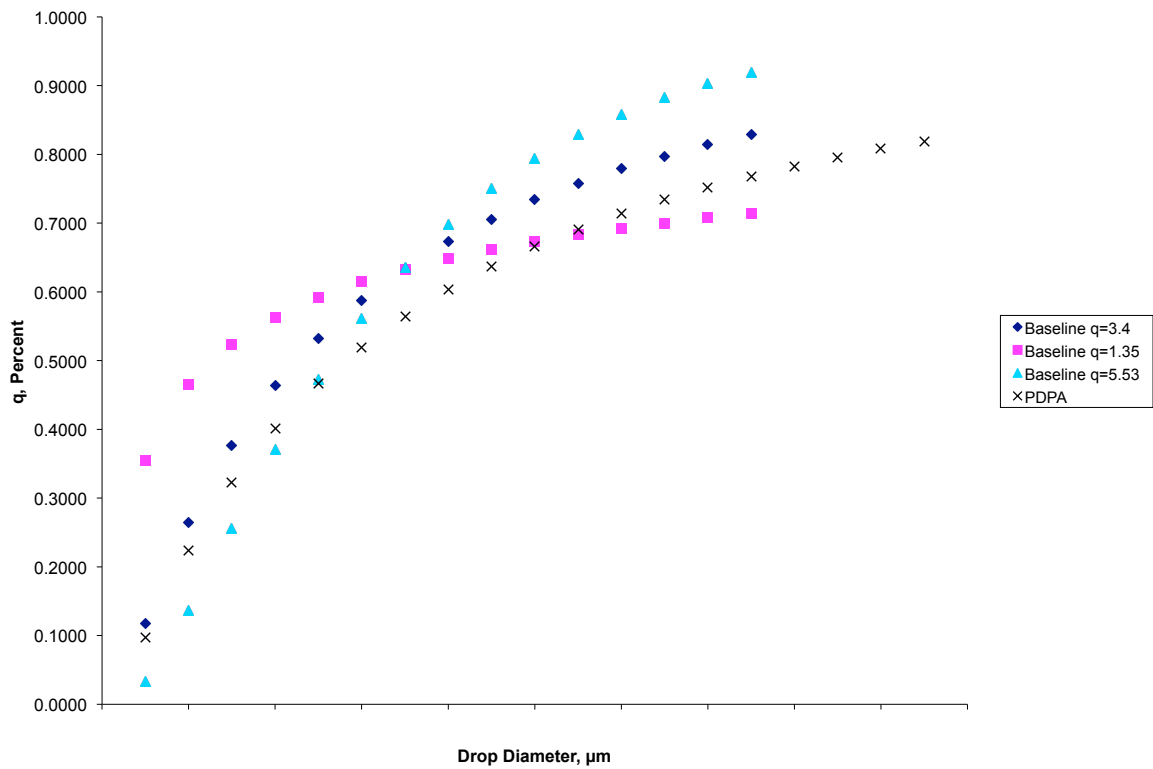


Figure 5.8: Varying the Spread of the Diameters -Baseline Conditions

Figure 5.9: Varying the Spread of the Diameters (q) -Modified Baseline Condition

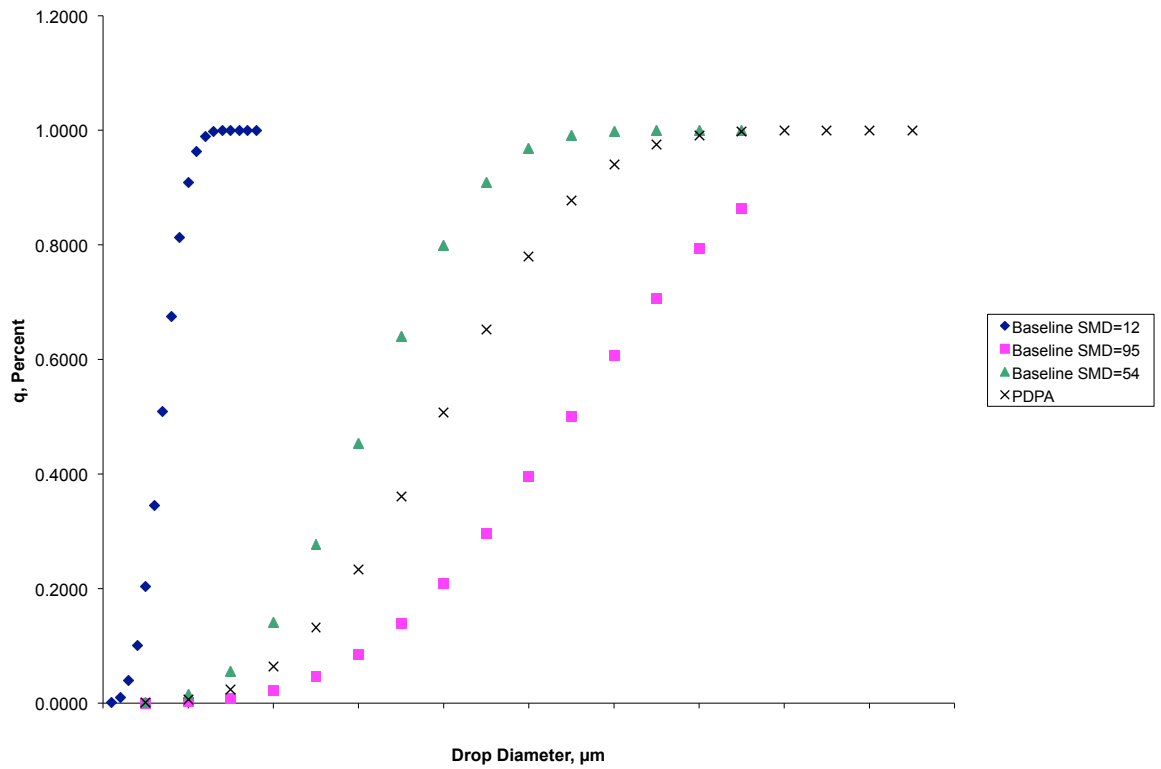


Figure 5.10: Varying the Sauter Mean Diameter – Baseline Condition

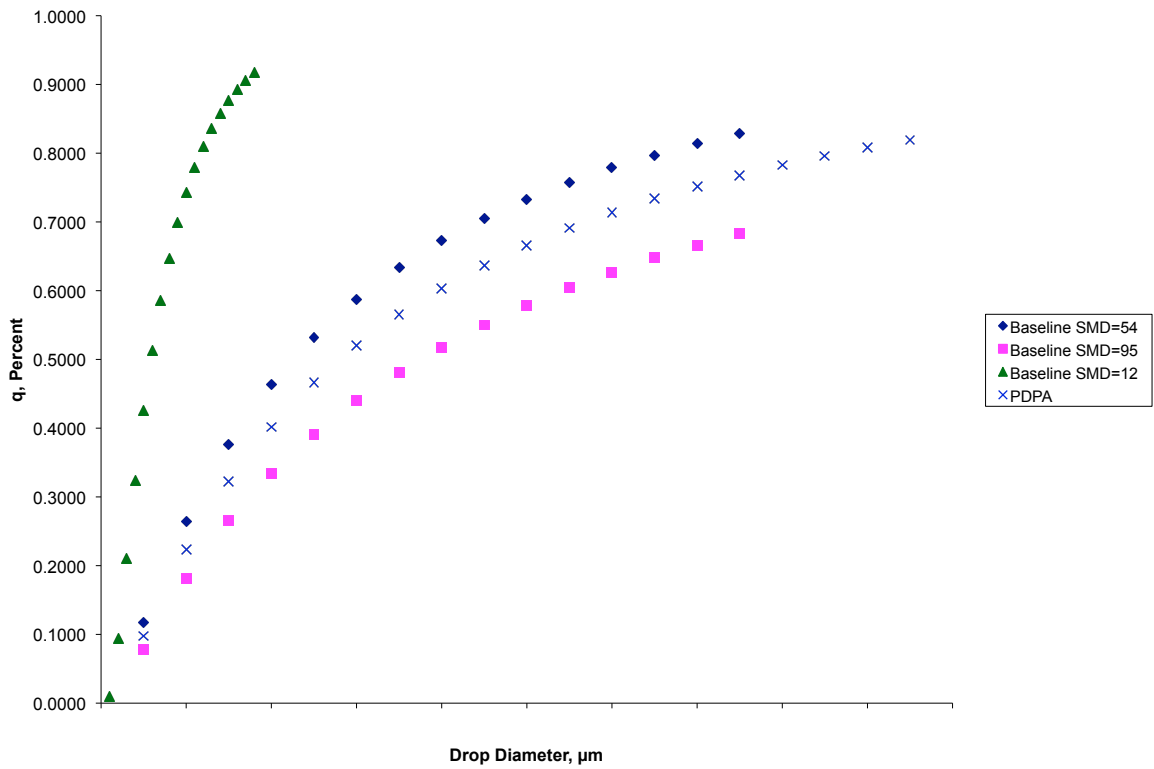


Figure 5.11: Varying the Sauter Mean Diameter-Modified Baseline Condition

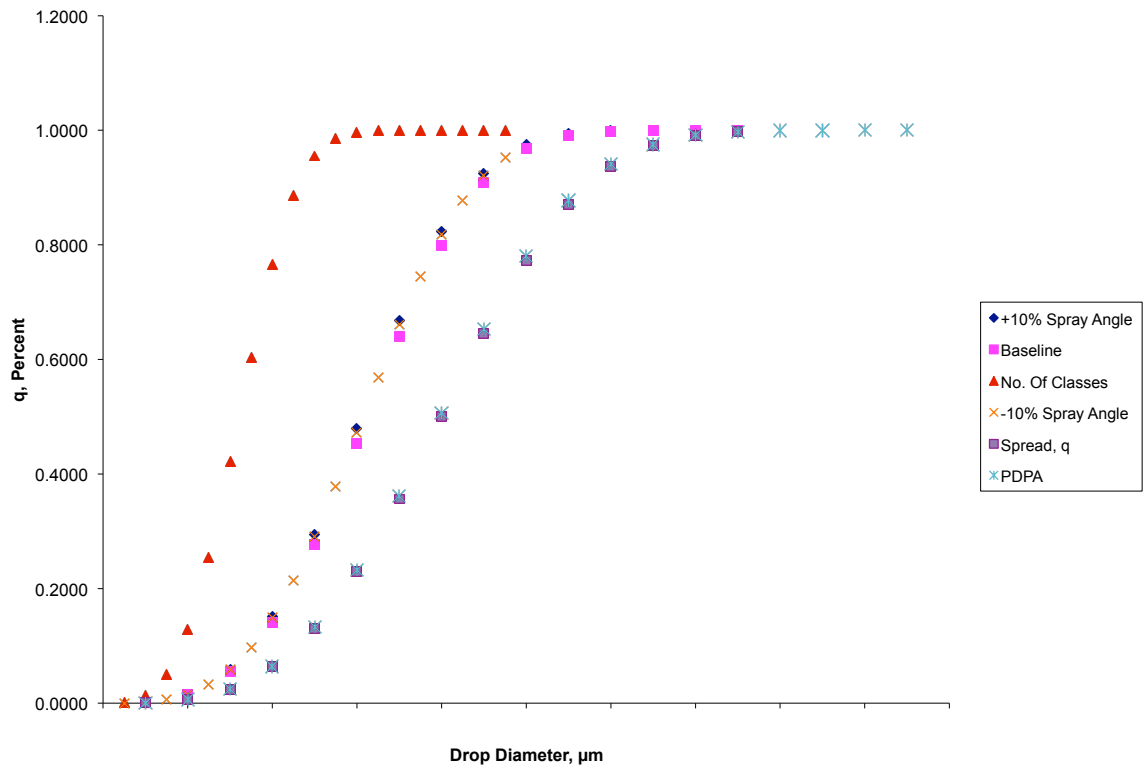


Figure 5.12: Rosin-Rammler Plots - All Spray Variations

5.12 . It was shown that increasing the number of diameters within the spray decreases the range of the drop diameters decreasing their maximum diameter and increasing the amount of drops with smaller drop sizes.

This figure 5.12 shows that changing the spray angle has little effect of the droplet diameters. Increasing the spread of the spray as expected increases the percentage of droplets with larger droplet diameters.

The PDPA data was well matched when the spray spread was set to 2 within the FLUENT simulation shown in Figure 5.12.

Velocity Plots

Another useful tool for analyzing the data was plotting the velocities against the radial length of the fuel's nozzle. This gave a picture of the spray in the radial, axial and tangential directions shown in Figure 5.13 - 5.15. Comparing the PDPA data with the baseline CFD results for the Axial direction, Figure 5.16, one can see that the profile of the FLUENT data had some similarities to the PDPA point's peaks and valleys. After examining the plots of the U,V, and W velocities, it was found that FLUENT does provide reasonable trends in the axial and radial velocities. However, there is a great offset with the axial velocities between the FLUENT and the PDPA data. The percentage of error between the two data sets has an average error percentage of 53.54%. The acceptable industry standard percentage of error is around 2% however this is a very hard percentage error to achieve with CFD software. The Radial direction is better having a percentage of error of 16.2% at -0.004mm from nozzle centre and 17.86% error at 0.003mm from the centre of the nozzle. The velocity found in the CFD results is highest at 20 mm from the centre of the nozzle, this could be attributed to the wall settings of the nozzle. These settings affect the turbulent boundary layer present on the nozzle's wall. This could cause the friction to be less than the actual and therefore increase the droplets velocity in the axial direction.

This large off set could be caused by how the Figures where created. The first step in post processing the CFD results was to rotate the co-ordinate system to match the radial, axial and tangential directions of the PDPA data. This was done using Euler Angles to transpose the co-ordinate system found in the FLUENT program to that used in the PDPA data. The CFD data was then post processed by finding the sum of all

the points at a certain distance along the radial axis of the nozzle. This is not an ideal method of comparing the results from FLUENT to the experimental data. The PDPA data is created by using a laser to measure one laser wide cross-section of the nozzle face. To replicate this and create a good comparison from the CFD results, a line of data across a cross section would need to be found that contains enough data within a laser beam width to compare with the PDPA data. The data that was collected from the CFD results was not able to provide this information. Therefore, the data was collected for all areas of the nozzle face and averaged.

There was no PDPA data collected for the tangential velocity. However, the variable data follows more or less the same profile, Figure 5.15. Changing the variables for this study affected the profile of the plots however, the overall magnitude of the velocities was not changed. This trend can also be seen in the plots for the radial and axial velocity vectors as well, as shown in Figures 5.13, and 5.14.

The above plots have been the average of each velocity at each point along the radial length of the fuel's nozzle. Figure 5.18 shows the plot of all the points collected through CFD for the Baseline Parameter variable. It can be seen that the plot is not perfectly symmetrical. This means that the velocities are not uniform over the face of the nozzle. This relationship can also be seen when looking at the physical distributions of the particles. The contour plots that show the number of particles passing through a particular area also show some unsymmetrical tendencies when the studies variables are changed. The Baseline plot in Figure 5.19 and the Diameter Spreads plot, Figure 5.23, illustrate a symmetrical droplet distribution were changing the sprays angle and the number of diameters do affect the drop distribution uniformity, which are shown in Figures 5.20, 5.21, 5.22. This could be attributed to the airflow of the nozzle as increasing or decreasing the spray angle subjects the droplets to a different air flow. Also, changing the drop diameters changes the mass of the drops and therefore allowing the air to have a greater effect on the drops affecting the uniformity of the distribution.

The unbalance of airflow from the fuel nozzle can be attributed to how the air enters the nozzle inlet. As seen in Figure 5.24, the nozzle is not located in the centre of the air-box, instead it is located at the end of the box. The inlet of the nozzle is an oval opening on one side of the nozzle. This means that it allows the air to enter at one side through a window in the nozzle and not uniformly over the diameter of the nozzle. This setup affects the nozzles performance as shown by the velocity vectors shown in Figure

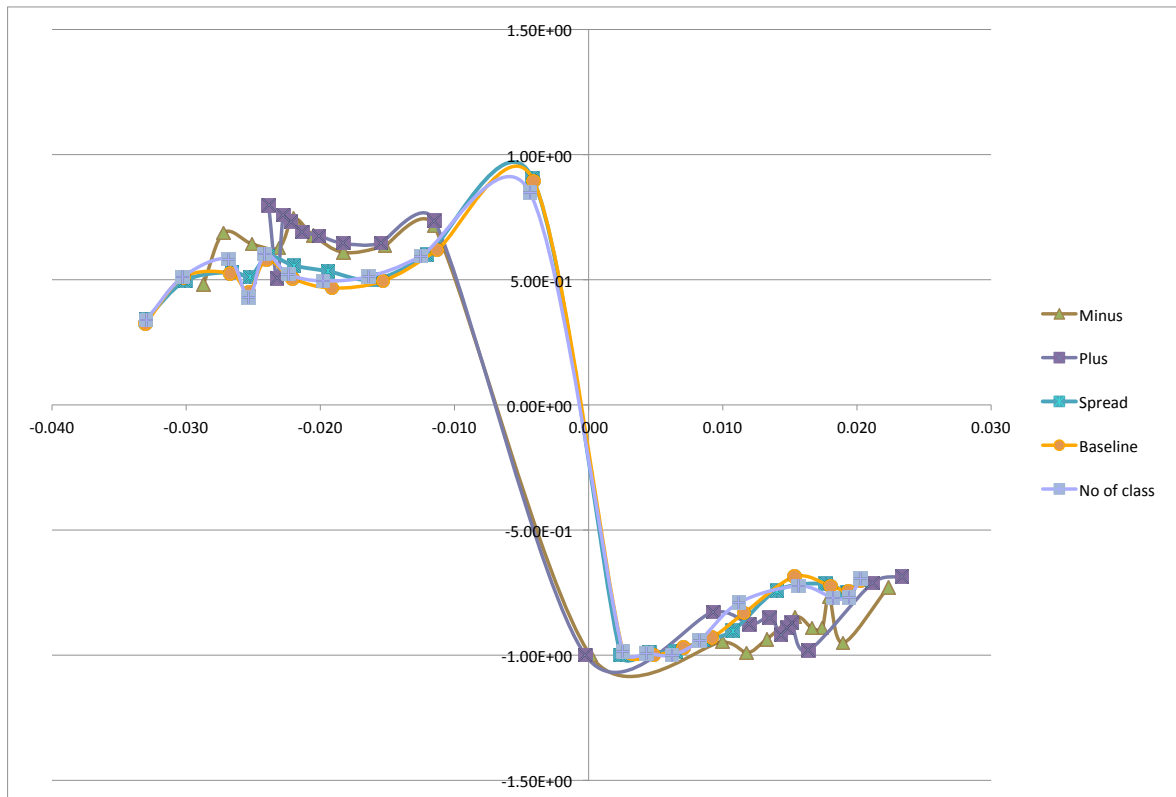


Figure 5.13: Mean Radial CFD Velocities Vs. the Radial Length of the Nozzle

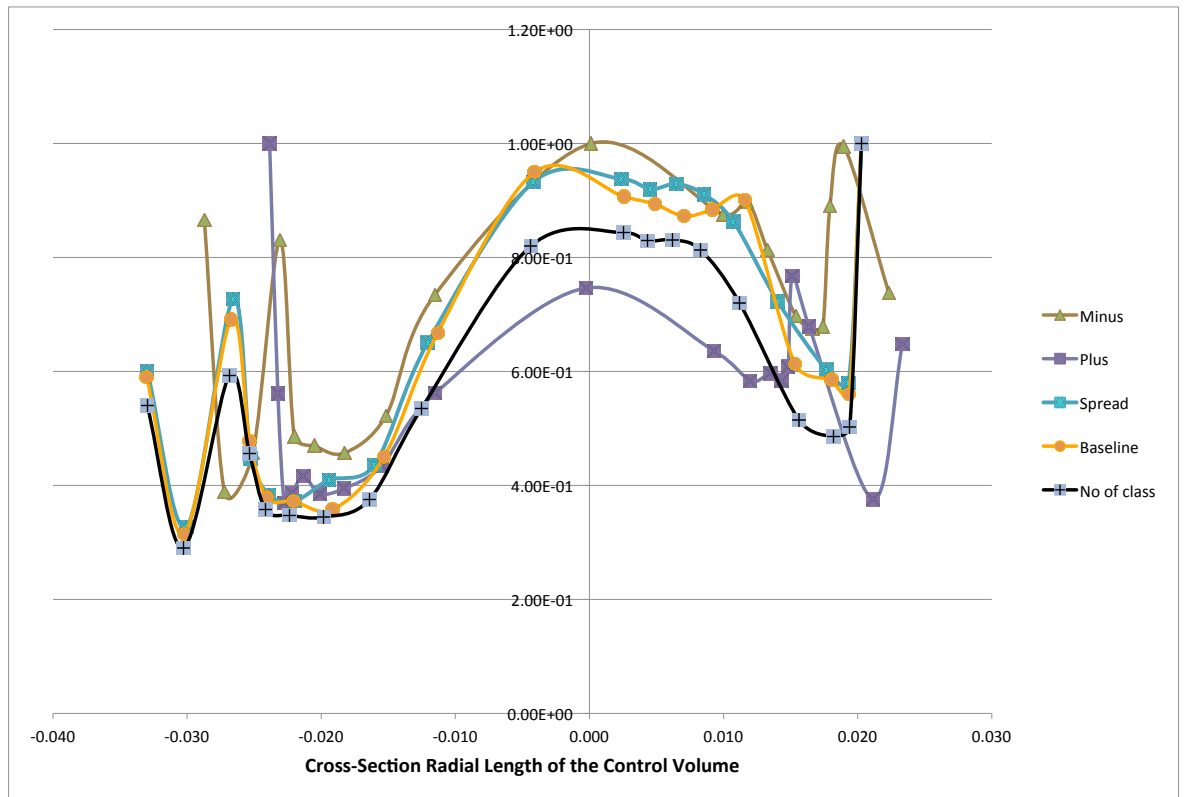


Figure 5.14: Mean Axial CFD Velocities Vs. the Radial Length of the Nozzle

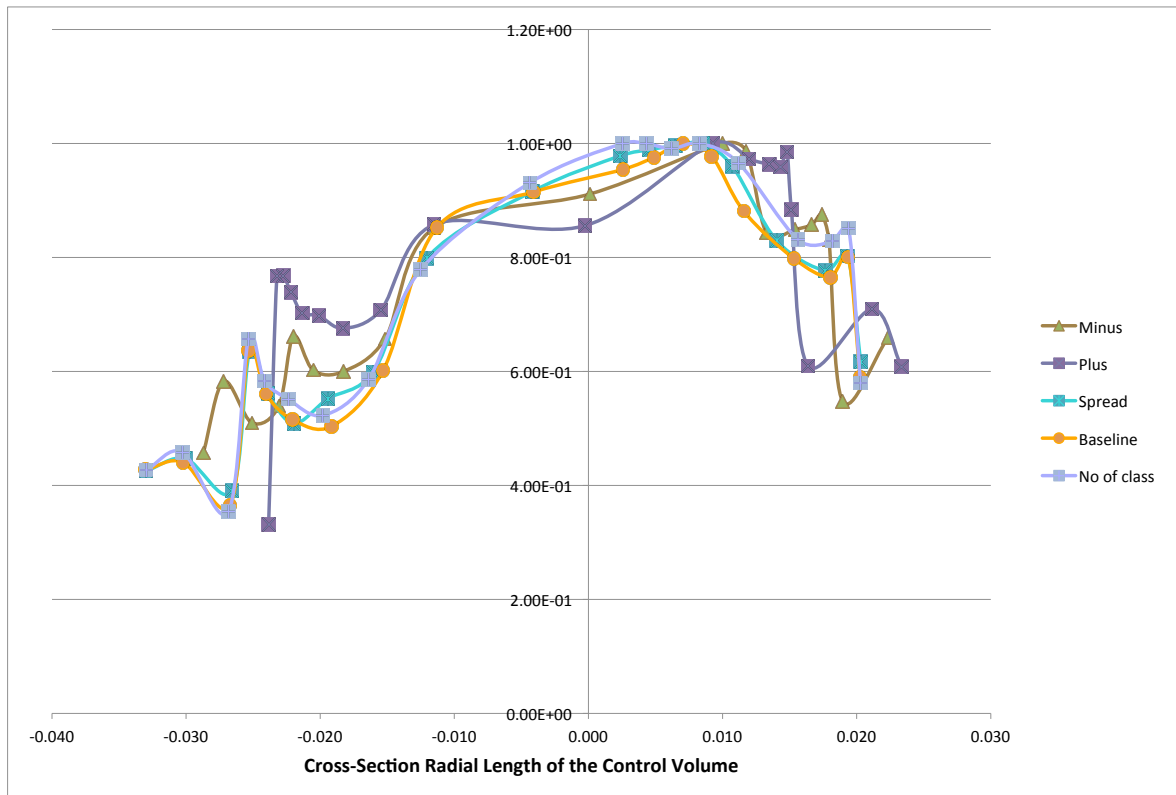


Figure 5.15: Mean Tangential CFD Velocities Vs. the Radial Length of the Nozzle

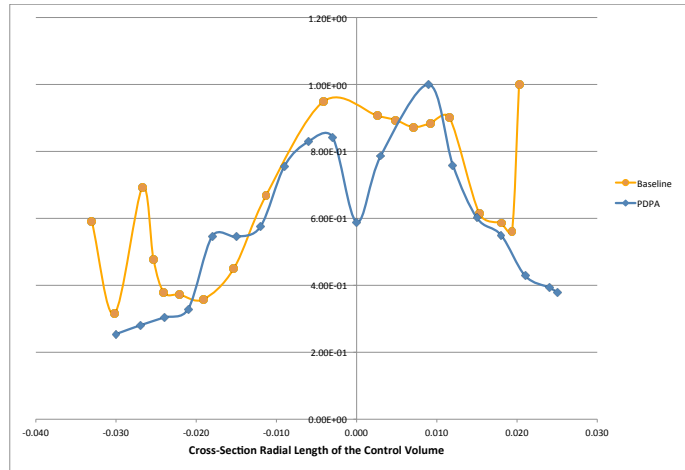


Figure 5.16: Mean Axial CFD Velocities Vs. the Radial Length of the Nozzle Vs the PDPA Results

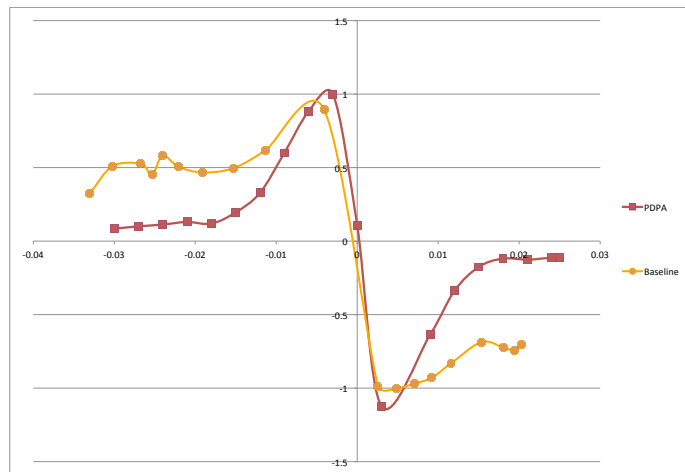


Figure 5.17: Mean Radial CFD Velocities Vs. the Radial Length of the Nozzle Vs the PDPA Results

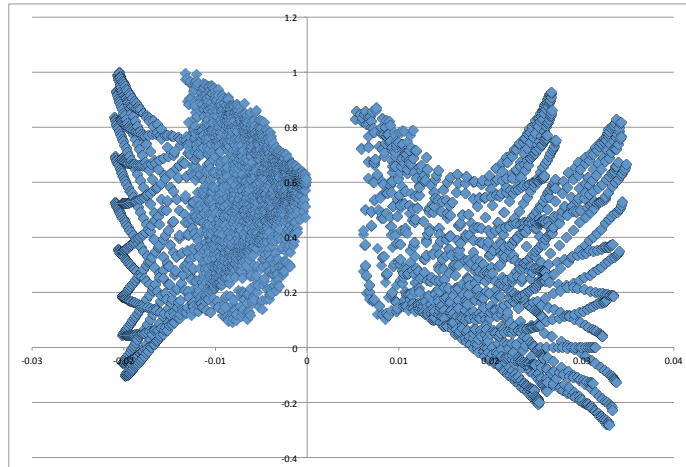


Figure 5.18: Unsymmetrical Mean Radial CFD Velocities Vs. the Radial Length of the Nozzle Plot- Baseline Parameter

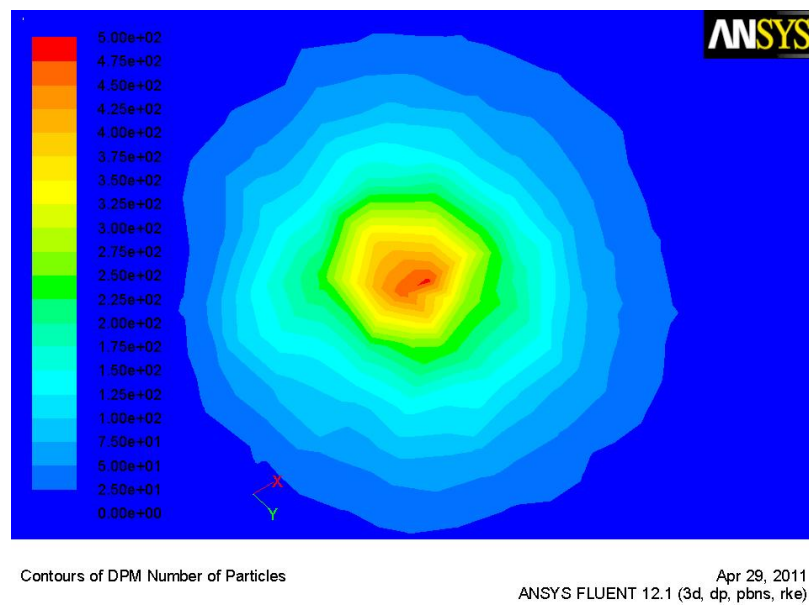


Figure 5.19: Contours of Number of Particles - Baseline Condition

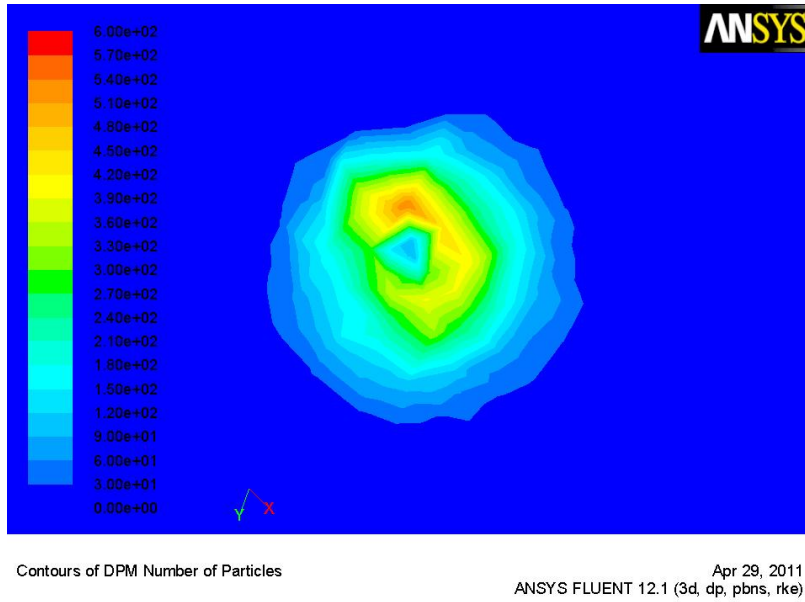


Figure 5.20: Contours of Number of Particles - Condition Reducing the in Initial Spray Angle By 10%

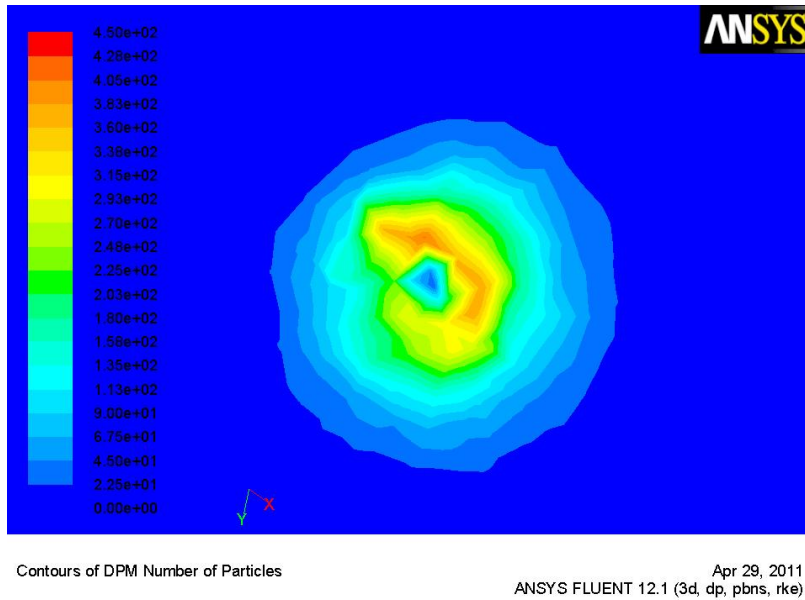


Figure 5.21: Contours of Number of Particles - Condition Increasing the Initial Spray Angle By 10%

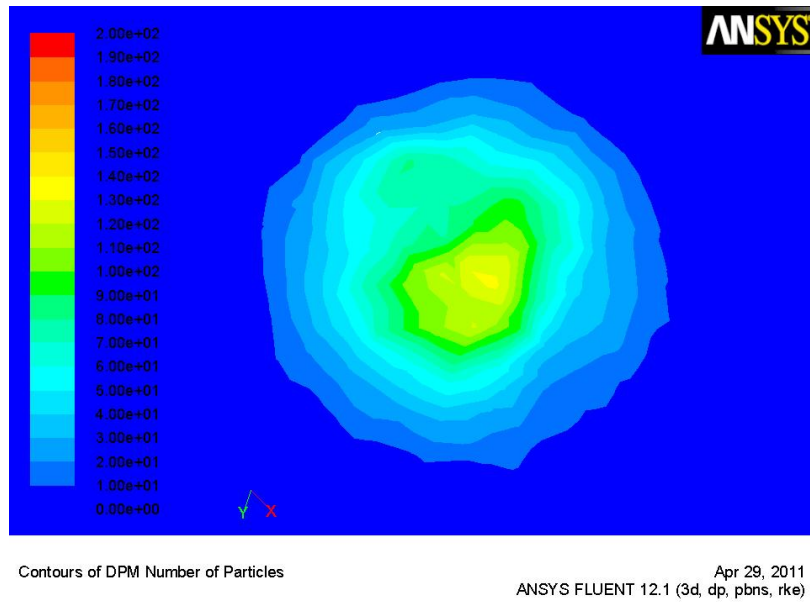


Figure 5.22: Contours of Number of Particles - The Rosin-Rammler Number of Classes Parameter

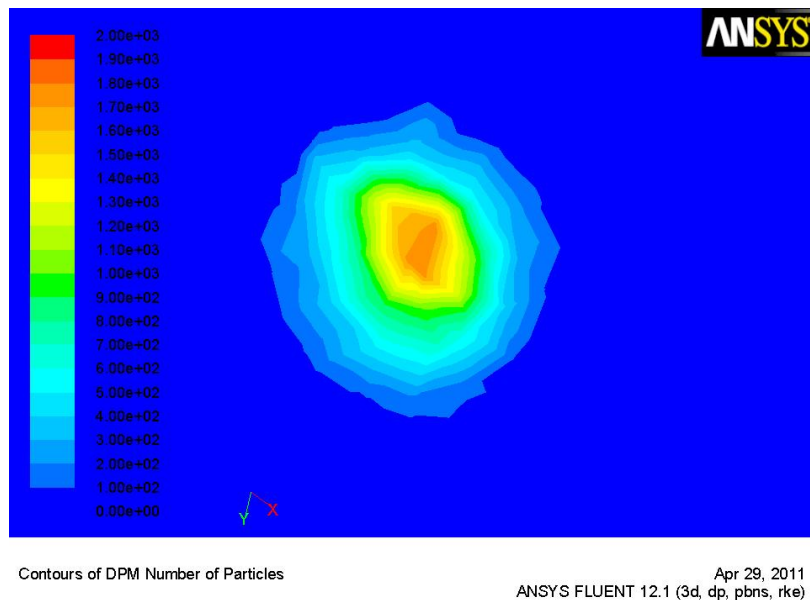


Figure 5.23: Contour of DPM Number of Particles – The Rosin-Rammler Spread Parameter



Figure 5.24: Air-Box cut away view

5.25. The plot in this Figure shows the circulating air forming because of the corners of the box. The velocity is also much higher around the entrance of the nozzle and along the left side of the nozzle as illustrated in Figure 5.27. The static pressures are also not uniform over the nozzle inlet, which could cause unbalance in the spray footprint, Figure 5.28.

Concentrations

Changing the angles of the spray greatly changes the concentration plot in comparison to the baseline plot, Figure 5.31,5.32, 5.29. This could be due to the airflow from the nozzle. Since these particles would interact with a different airstreams developed by the nozzle, the particles would take a different path through the control volume. This means that the increase in spray angle could cause less of the spray to be caught up in the central recirculation flow. This would create a more even concentration distribution in the plot with less concentration in the centre of the spray and a more even concentration around

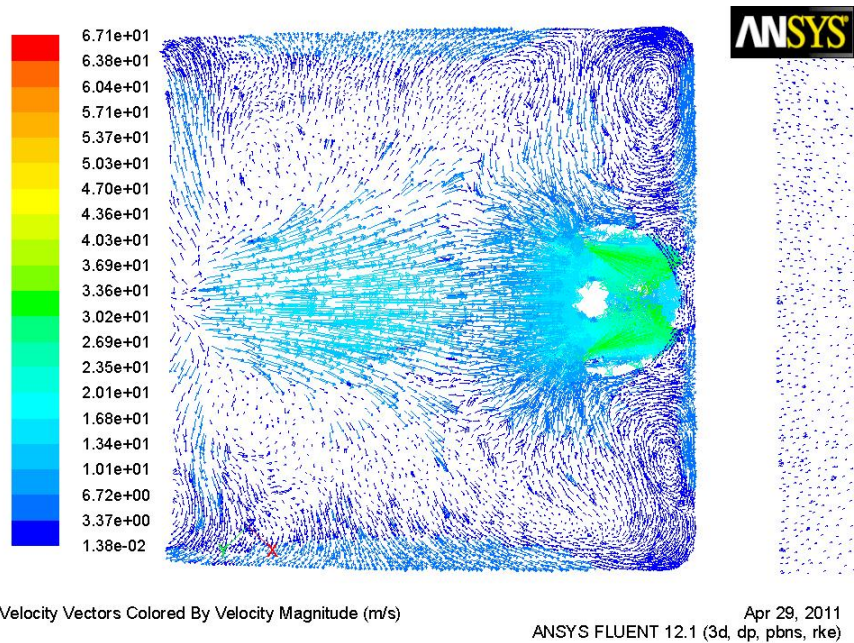


Figure 5.25: Air-Box Velocity Vectors

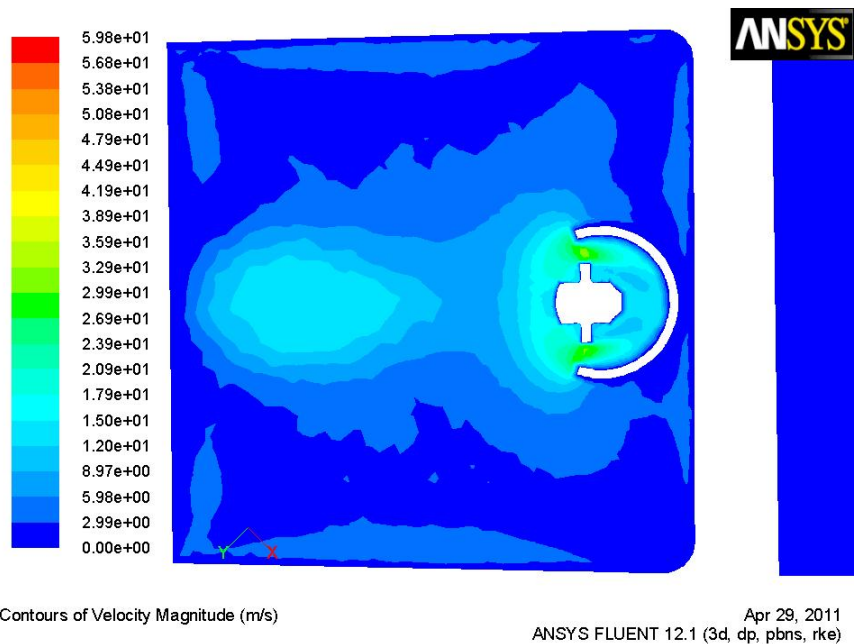


Figure 5.26: Air-Box Velocity Contours

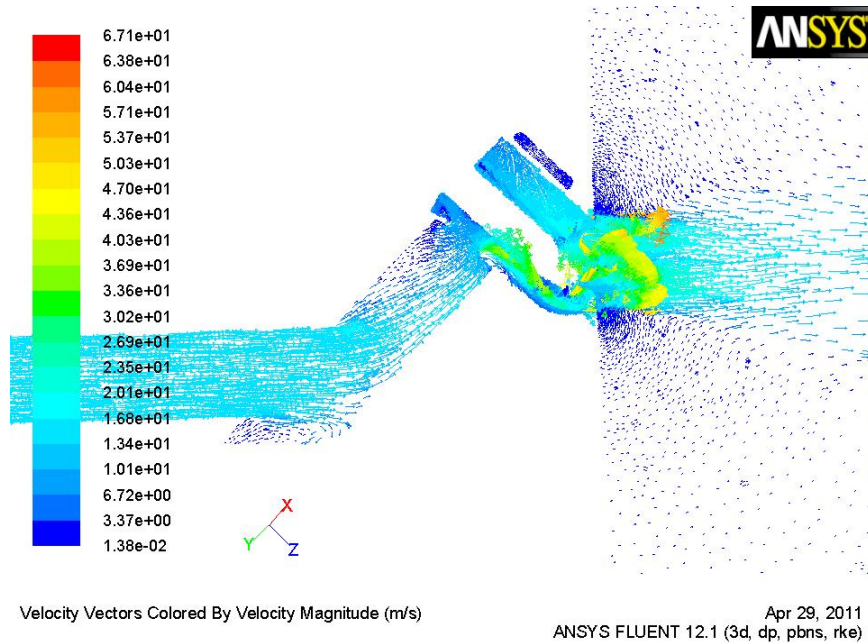


Figure 5.27: Axial View of Nozzle - Velocity Magnitude Plot

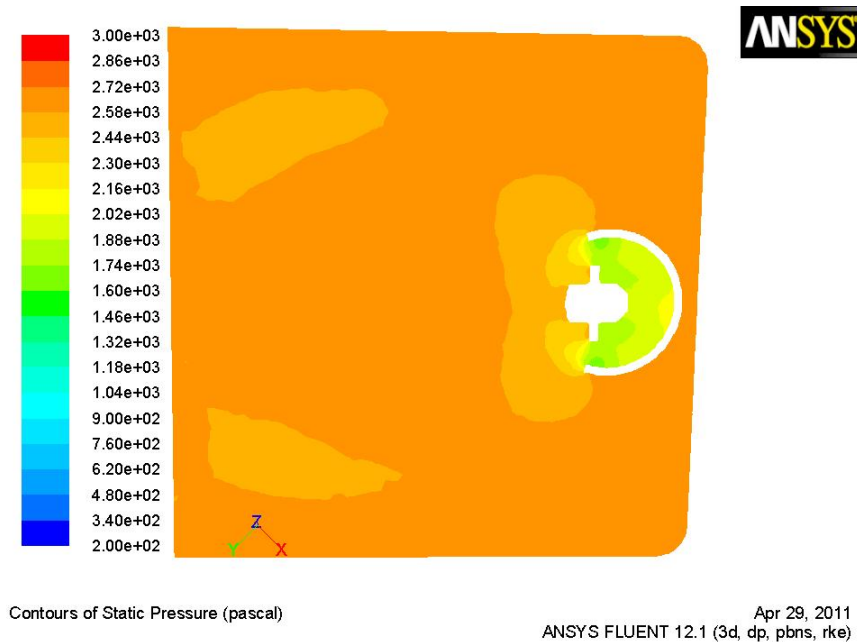


Figure 5.28: Air-Box Pressure Contours

the outer regions. Reducing the spray angle could cause more of the flow to get caught in the inner recirculation flow and therefore a less concentrated flow would be shown in the concentration plot at one inch from the nozzle face. This results in a slight change in the concentration plot in Figure 5.33 showing an increase in the number of diameters in a certain area of the control volume. Increasing the number of diameters within a spray will cause a change in the amount of particles that are in a certain area within the control volume, which means changing the concentration, or refining the concentration plot allowing for more slight changes in the spray concentration to be more noticeable. Reducing the spread, which makes the spray less uniform, provides a more uniform concentration plot, 5.30.

This data compares well to the patterning data, which was collected from a mechanical rig known as the patternator. An explanation of this rig can be found in Section 2.3.2. The patterning collection area is broken up into many annuli as shown in Figure 5.34. The graphs shown below, Figures 5.35, 5.36 and 5.37, are the percentage of fuel present in each of these annuli verses the annuli number the fuel is found in. The graphs show different cross-sections of the patterning area to illustrate the distribution across different areas of the nozzle. The patterning data shows that the largest amount of the fuel is collect in the centre of the nozzle and the concentration decrease as the distance from the centre increases. The same trend is found in the FLUENT contour plots taken 1 inch from the nozzle face.

Since Figure 5.35, Figure 5.36 and Figure 5.37 are different, this echoes the findings that the flow is not symmetrical from one side of the nozzle to the other, and therefore the CFD simulation was correct in that prediction. Since the contour plots do not show perfect circles of decreasing concentrations, there are variations in the concentration distribution. However, there are cross-sections that can be taken that show a more linear relationship between distance and concentration as in Figure 5.36.

The patterning data is taken at a distance of 1.5 inches from the nozzle face. Therefore, a sample of droplet data was found for a plane that is 1.5 inches from the nozzle face. This data showed very different results, Figure 5.38.

These numbers may be so off from the mechanical results with an average error of 74%, for a couple reasons. First, the post processed results are the sum of all the points at a certain distance along the radial axis of the nozzle. This is not an ideal method of comparing the results from FLUENT to the mechanical rig data. However, it is hard to

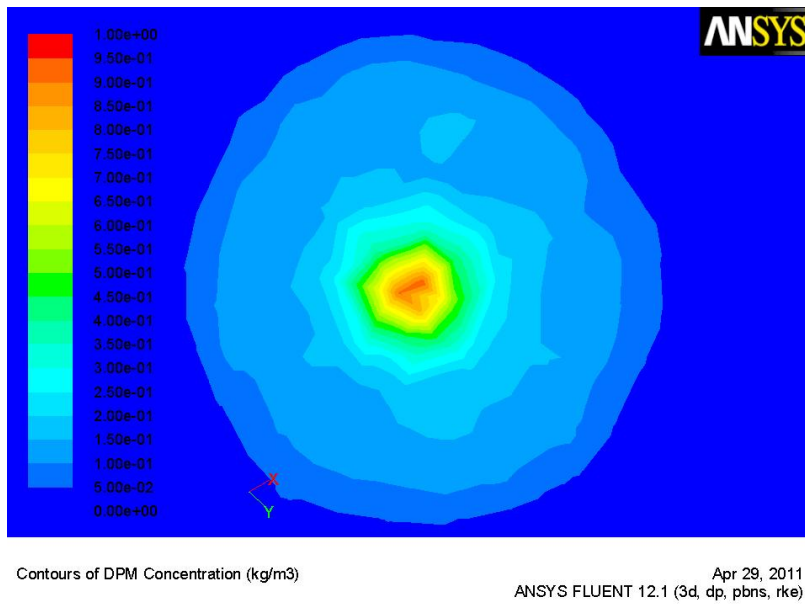


Figure 5.29: Contours of Concentration - Baseline Condition

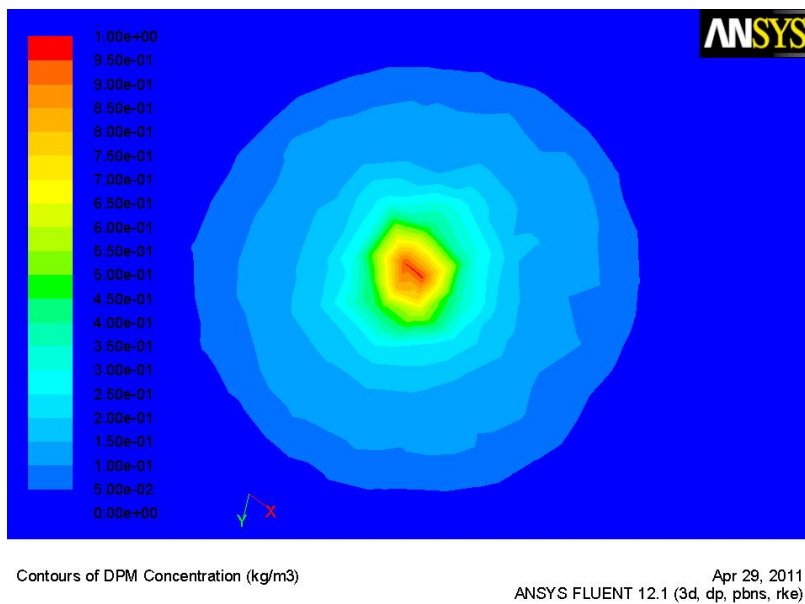


Figure 5.30: Contours of Concentration - The Rosin-Rammler Spread Parameter

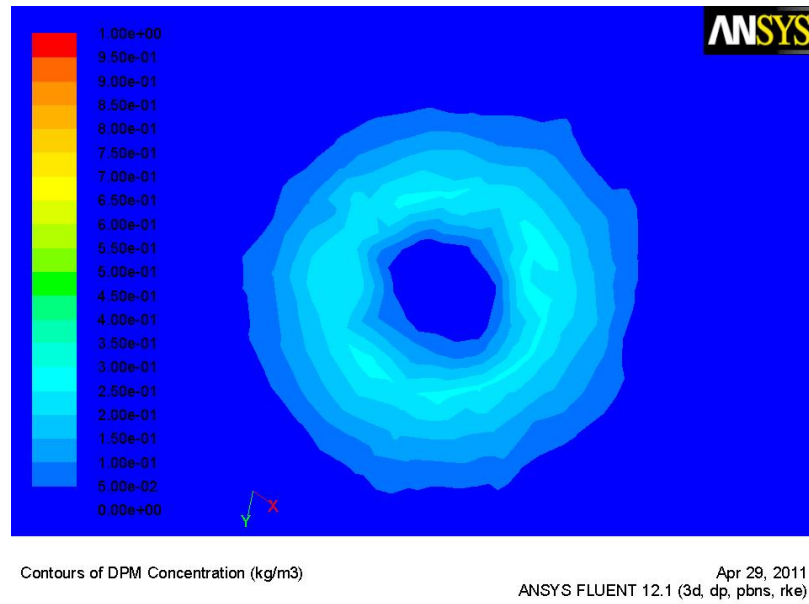


Figure 5.31: Contours of Concentration - Condition Increasing the Initial Spray Angle By 10%

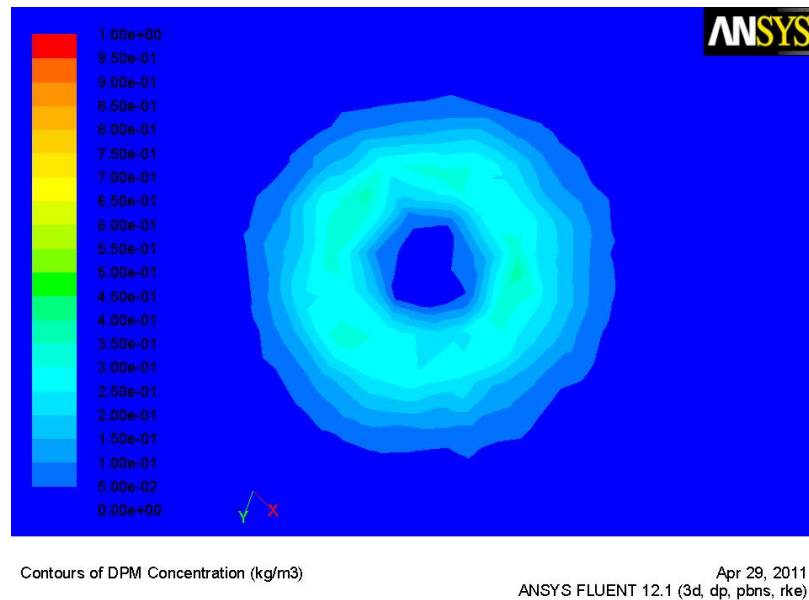


Figure 5.32: Contours of Concentration - Condition Reducing the in Initial Spray Angle By 10%

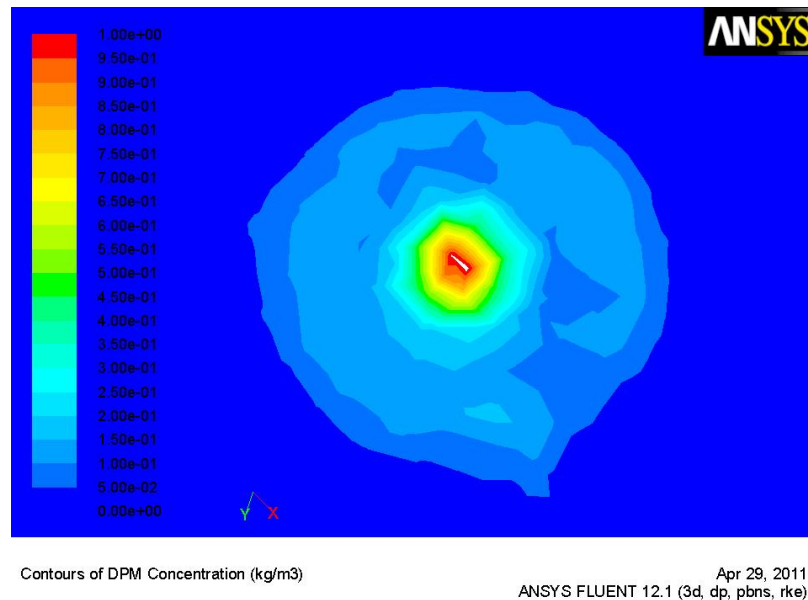


Figure 5.33: Contours of Concentration - The Rosin-Rammler Number of Classes Parameter

isolate the different annuli and come up with a percentage that each annuli contains. This is due to the fact that FLUENT provides the user with a very large sample of droplet information in text form. An example is the xyz co-ordinates. The concentration plots shown provide a much better representation of the data.

Secondly, the off set of the data could be due to the recirculation region, which is discussed below, might be smaller than that of the mechanical rig. The numbers match better at a distance of 1 inch than they do for a distance of 1.5 inches because once the droplets reach a distance of 1.5 inches from the nozzle the concentration of the spray much less in the nozzles centre, for example for the baseline case the centre region on the plane 1.5 inches from the nozzle face contains about half of what was found 1 inch from the nozzle face. This can be seen in the concentration plots taken at a distance of 1.5 inches from the nozzle face shown in Appendix A.

Particle Tracking

The recirculation zone in the middle of the spray can be seen in Figure 5.39. This zone is created to keep the spray in that location, which is close to the igniter, for as long as

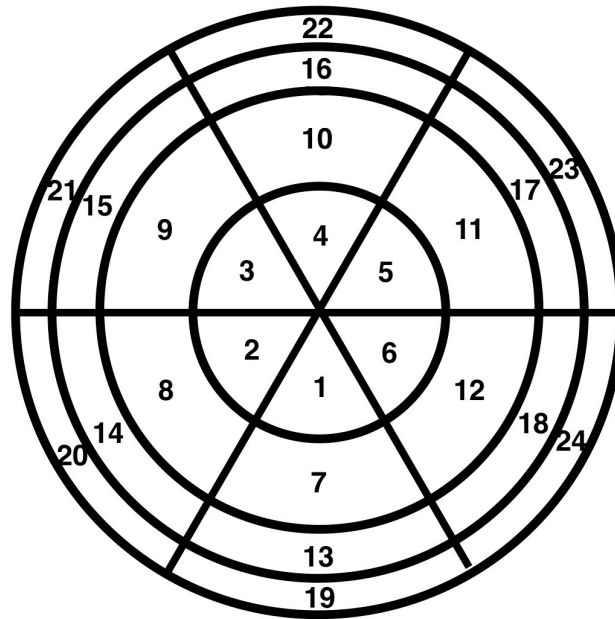


Figure 5.34: Patteration Annulus Collector Diagram

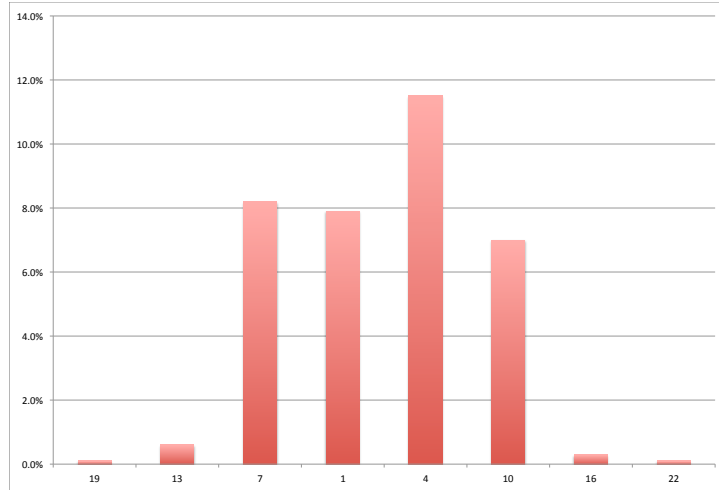


Figure 5.35: Percentage of Fuel Mass Vs. Radial Length Cross-Section 1

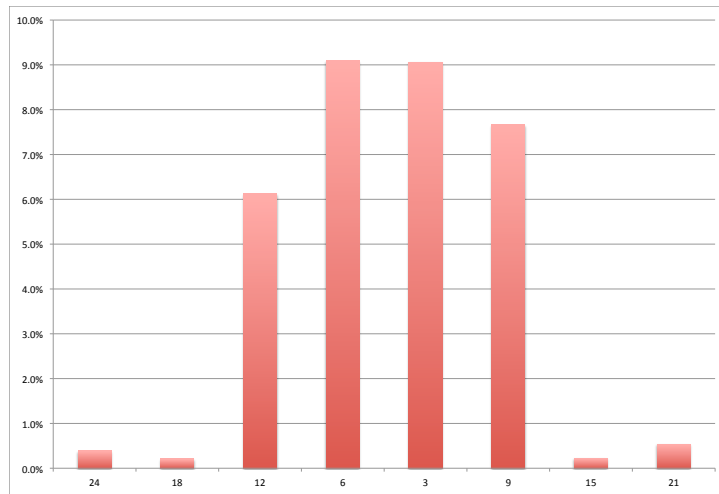


Figure 5.36: Percentage of Fuel Mass Vs. Radial Length Cross-Section 2

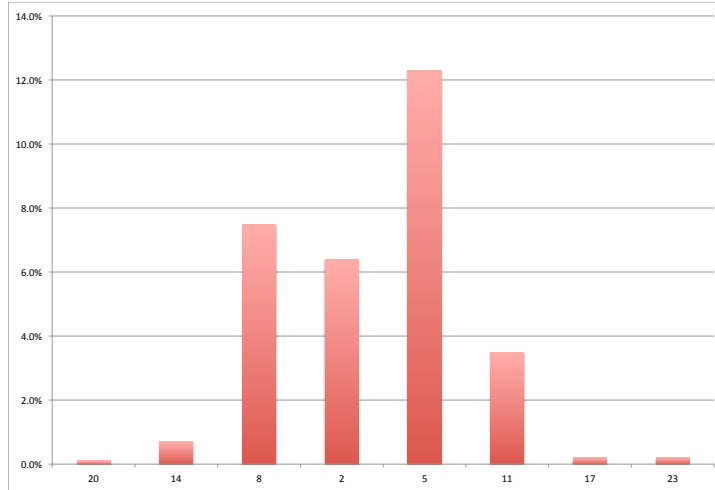


Figure 5.37: Percentage of Fuel Mass Vs. Radial Length Cross-Section 3

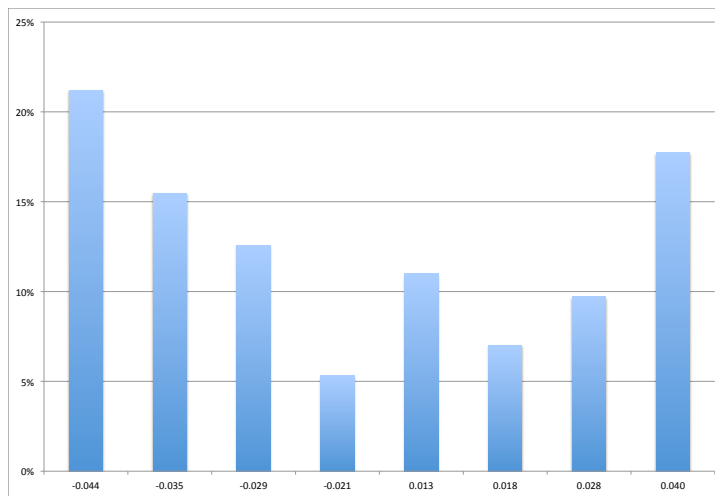


Figure 5.38: Percentage of Fuel Mass Vs. Radial Length Cross - Baseline Conditions

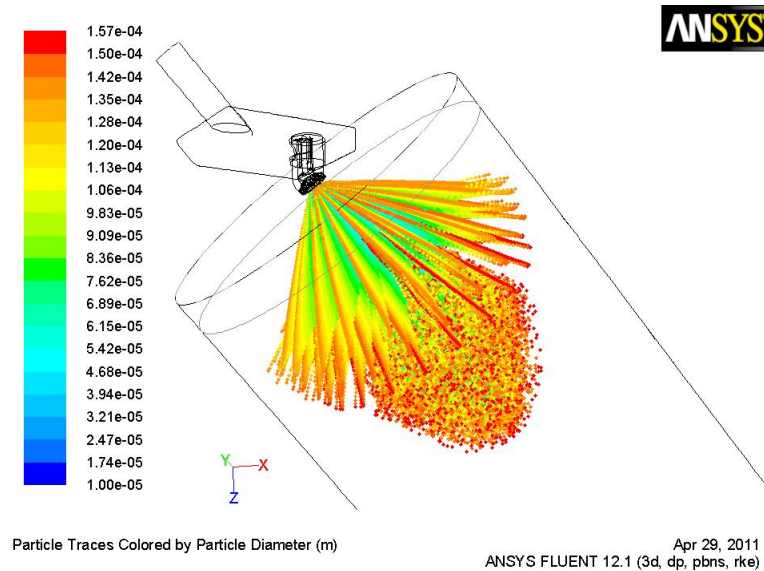


Figure 5.39: Particle Traces Colored by Particle Diameter (m) - Baseline Condition

possible to ensure better ignition. It can be seen in Figure 5.39 that the larger particle sizes are forced to the outside, and the smaller diameters are caught up in the inner airflows and recirculated back towards the nozzle.

Reducing the spray angle increases the amount of smaller particles, which are then caught up in the recirculating flow. This is shown in Figure 5.41, as the smaller amount of particles are down stream of the nozzle. The strength of this recirculating flow is shown in Figure 5.42. The larger particles are being pulled in closer to the core than what was found in the baseline condition. Figure 5.42 also shows that the spray is in fact being injected at a reduced angle which helps validate the model.

Increasing the spray angle also gives similar results as shown in Figures 5.43, 5.44. The larger particles are in the mid part of the spray due to the interaction of the spray outward force and the recirculating inner forces. The injection is injected at a larger angle again helping to validate the results.

The particle track plot for the variable changing the number of diameters within the spray is very different from the rest of the CFD results, as shown in Figure 5.47 and Figure 5.48. The spray appears to be smaller than the others and more uniform in diameter and consequentially in mass.

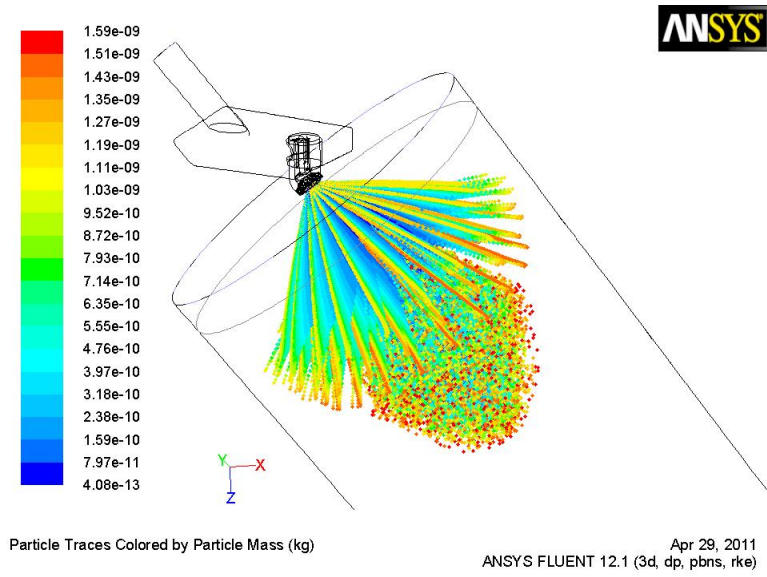


Figure 5.40: Particle Traces Colored by Particle Mass (kg) - Baseline Condition

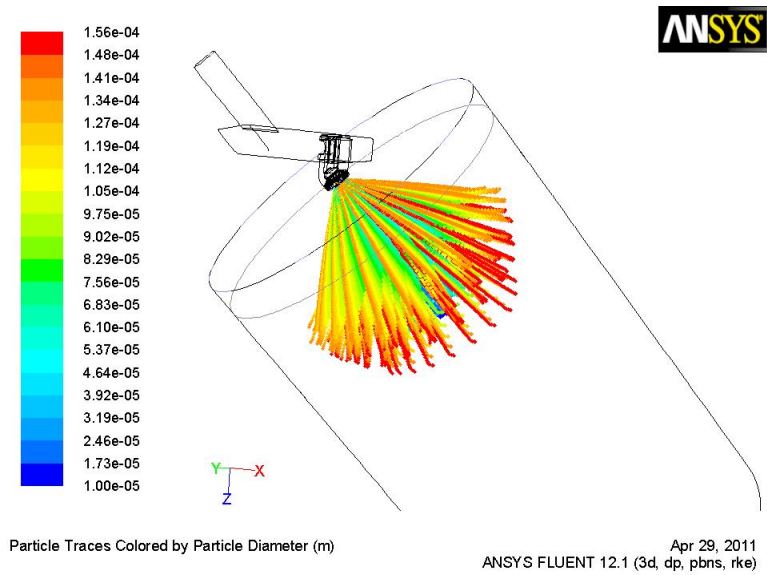


Figure 5.41: Particle Traces Colored by Particle Diameter (m)- Condition Reducing the in Initial Spray Angle By 10%

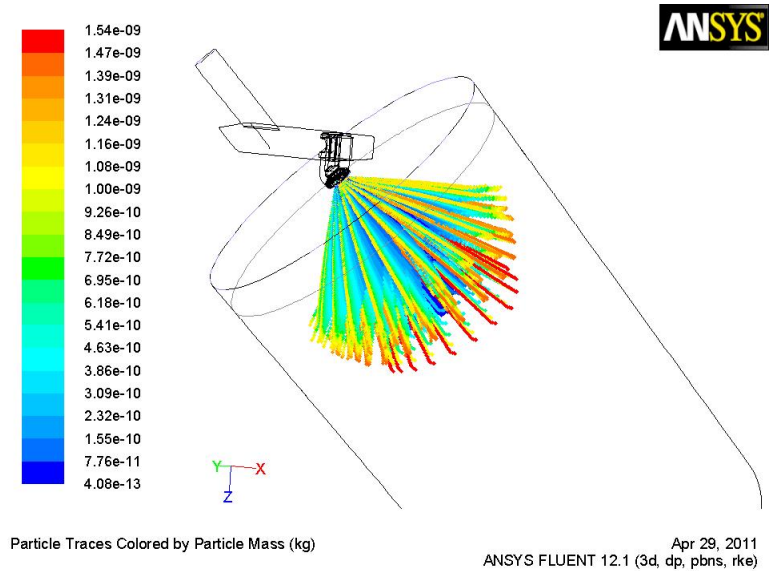


Figure 5.42: Particle Traces Colored by Particle Mass (kg)- Condition Reducing the in Initial Spray Angle By 10%

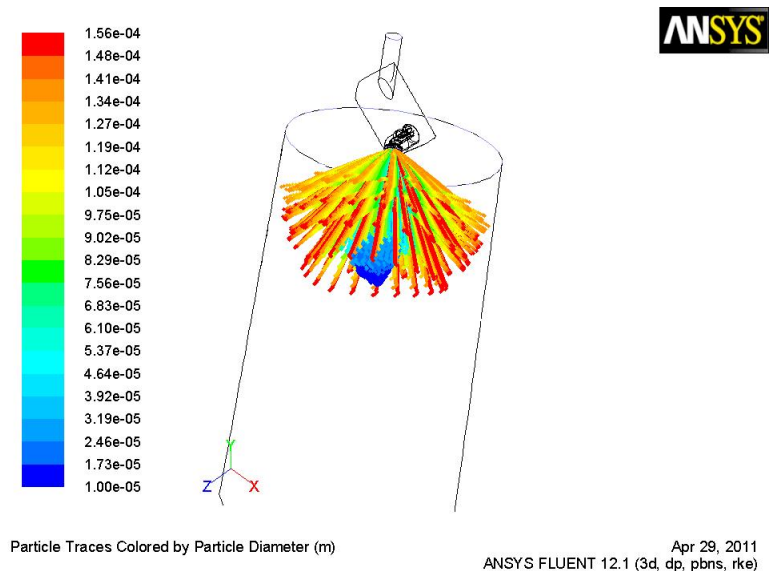


Figure 5.43: Particle Traces Colored by Particle Diameter (m)- Condition Increasing the Initial Spray Angle By 10%

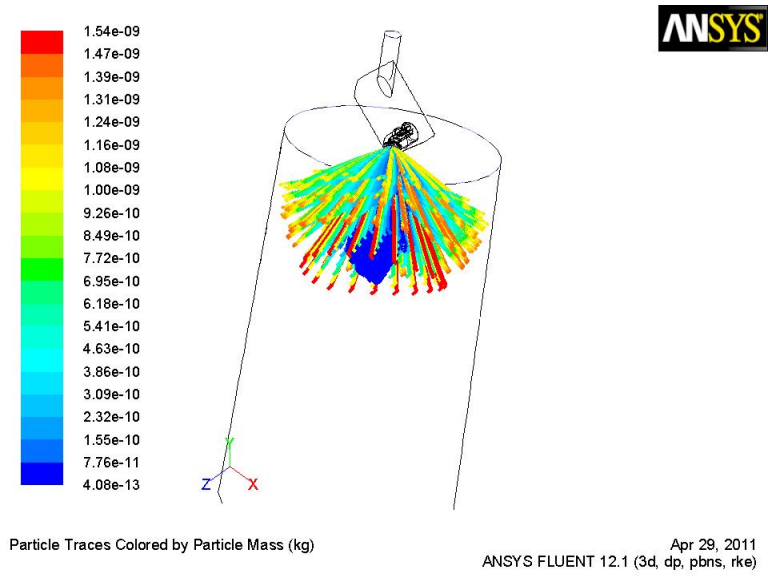


Figure 5.44: Particle Traces Colored by Particle Mass (kg) - Condition Increasing the Initial Spray Angle By 10%

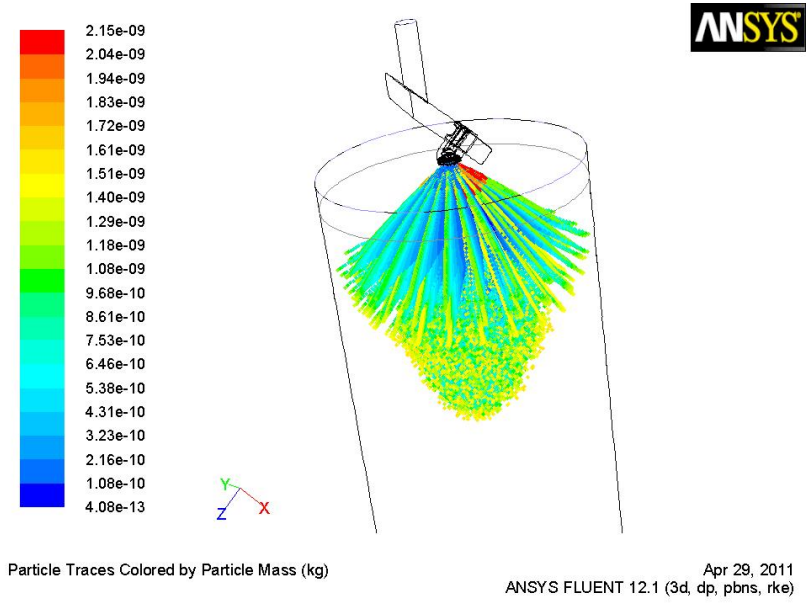


Figure 5.45: Particle Traces Colored by Particle Diameter (m) - The Rosin-Rammler Spread Parameter

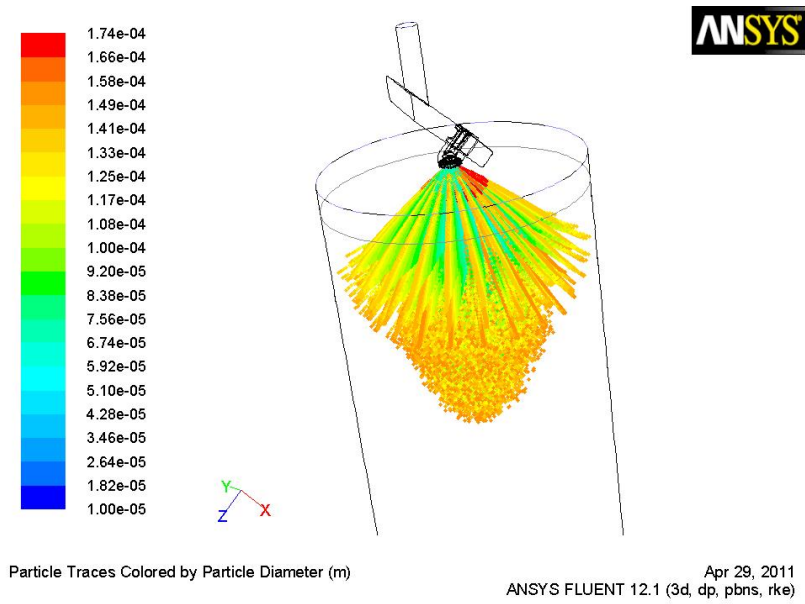


Figure 5.46: Particle Traces Colored by Particle Mass (kg) - The Rosin-Rammler Spread Parameter

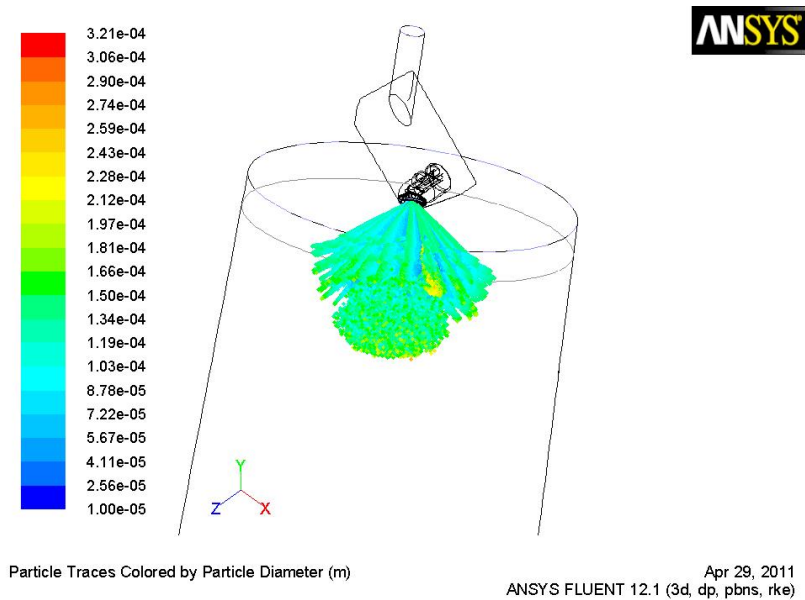


Figure 5.47: Particle Traces Colored by Particle Diameter (m) - The Rosin-Rammler Number of Classes Parameter

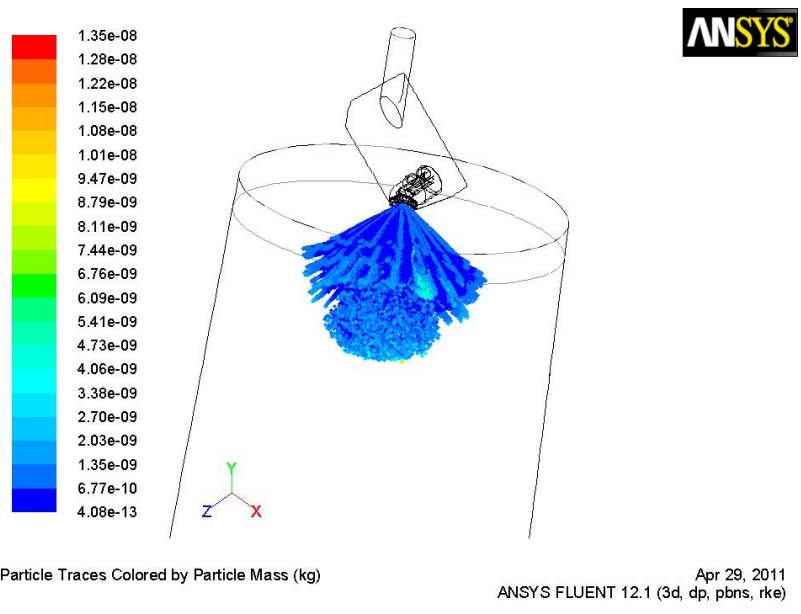


Figure 5.48: Particle Traces Colored by Particle Mass (kg) - The Rosin-Rammler Number of Classes Parameter

Chapter 6

Conclusions and Future Work

6.1 Conclusions

The FLUENT software is a new tool in the aerospace industry. This tool provides the industry with combustion modeling capabilities never had before. Validating this software against known test data is useful in testing this softwares capabilities and findings its limitations so that its capabilities can be used to its full extent.

This study demonstrates that each input parameter into the simulation has a unique and dramatic affect on the simulation's output and its correlation with the physical data. However, more importantly, it was the creation of a realistic simulation, incorporating all the complexities of spray injection, that would result in a good correlation with the physical data.

A numerical model using the Fluent software was produced to simulate the spray distribution. The results of this model have been compared to data collected from the mechanical rig. A parametric study has been preformed on the model variables to identify the sensitivities of these parameters on the spray characteristics.

The variables that were considered were the Rosin-Rammler parameters, the initial number of diameters contained within the spray, the initial diameters of the droplets and the initial spread parameter. The initial angles to which the spray is injected was also increased and decreased by 10 percent.

The first comparison to the mechanical data that was made was the results of plotting the Rosin-Rammler plot. The variables discussed above proved to vary only with the

number of diameter classes used and with varying the spread of the diameters used. Increasing or decreasing the spray angle proved to not alter the Rosin-Rammler plot from the baseline values.

To experiment with the effects of changing the SMD and the percentage of droplets below a certain diameter, Q , these values were changed for the baseline case to better estimate the best values to use to achieve the PDPA results. It was found that altering these values did effect the Rosin-Rammler plot however a match to the PDPA data was not achieved. An attempt was used to use the modified Rosin-Rammler equation to provide a match to the PDPA data. This also did not provide a match. A match was achieved when the initial spread of the diameters used within the spray was changed to 2.

The next comparison was the velocity of the droplets. After examining the results it was found that changing the variables in question did not alter the out come of the results as much as was expected. The variable results all follow a similar profile. It was found that changing the initial angle of the spray reduced the velocity in the radial direction. Increasing the angle reduced the axial velocity where decreasing the initial spray angle increased the axial velocity. The tangential velocities showed a very similar profile for all variables.

After examining the plots of the U,V, and W velocities, it was found that FLUENT does provide reasonable trends in the axial and radial velocities. However, there is a great offset with the axial velocities between the FLUENT and the PDPA data. The percentage of error between the two data sets has an average error percentage of 53.54%. The acceptable industry standard percentage of error is around 2% however this is a very hard percentage error to achieve with CFD software. The Radial direction is better having a percentage of error of 16.2% at -0.004mm from nozzle centre and 17.86% error at 0.003mm from the centre of the nozzle. Therefore it was also found that the initial assessments of the spray parameters provide reasonable trends in the axial and radial velocities.

Some of the plots for comparing the velocity's discussed above displayed plots that there not symmetrical about the y-axis. This was thought to be attributed to the airflow into the nozzle. The air-box is a square box that surrounds the nozzle inlet area. The sharp corners of the box creates vorticities that disrupts the flow of the air into nozzle. The air inlet into the nozzle is an oval window on one side of the nozzle and does not allow the air to cover the diameter of the air passages evenly that could possibly create

uneven airstreams leaving the nozzle. This uneven footprint is seen in the contour plots showing the distribution of the particles.

The concentration plots proved to be very different for each of the variables included in this thesis. Reducing and increasing the initial angle of the spray injection reduced the amount of fuel found in the centre of the nozzle. Varying the initial number of diameter's otherwise known as the diameter classes or changing the spread of the diameters used proved to not show a great difference from the baseline case.

It was also found that the concentration plots taken at a plane 1.0 inches from the fuel nozzle compare well with the patteration data collected. The plots taken 1.5 inches from the nozzle face showed the concentration halved from that found in the later plane. This was thought to be due to the the plane 1.5 inches from the nozzle face being farther away from the recirculation zone and there fore showing a less concentrated area. This area was thought to be shorter for the CFD results due to the data found.

The forces produced on the spray by the airstream greatly affects the spray distribution and the location of the droplets. It was shown in the particle tracking plots, that the bigger droplets are forced outward in the baseline condition and kept closer to the centre when the spray has a narrower spray angle or a wider spray angle. It was shown that changing the number of diameters within the spray created a smaller more uniform spray in diameter and consequentially in mass.

After performing the literature review for this thesis it was found that there is little research done using FLUENT to model spray. Further a paper by M.G. Giridharan et al, was found concluding that the major issue that arose was specifying the initial conditions that accurately mirrored the laboratory conditions. This thesis's contribution to the industry is that it provides a parametric study of the challenging initial conditions that modeling spray involves. This study works to shed some light into how varying thesis initial conditions affects the end result of the CFD results. The hope is that this thesis provides more information to the industry on these estimated values and helps to improve the estimates used and therefore can be used to tune future spray models to better reflect the real spray model.

6.2 Future Work

This study will be useful for engineers to tune the spray model to predict the measured data from the patternation and Phase Doppler Particle Analysis (PDPA). Future work could include using scaled up data closer to operating conditions and comparing them to the FLUENT results until full engine conditions can be obtained. This will allow better predictions of the combustion within an engine in terms of emissions, both gaseous and particulate, temperatures, pressures, flame stability along with a myriad of others.

This could be done by using a multi-disciplinary optimization software to back calculate the initial conditions to input into the FLUENT software.

Appendix A

Concentration Plots Created On a Plane 1.5 Inches From the Nozzle Face

APPENDIX A. CONCENTRATION PLOTS CREATED ON A PLANE 1.5 INCHES FROM THE NOZZLE FACE

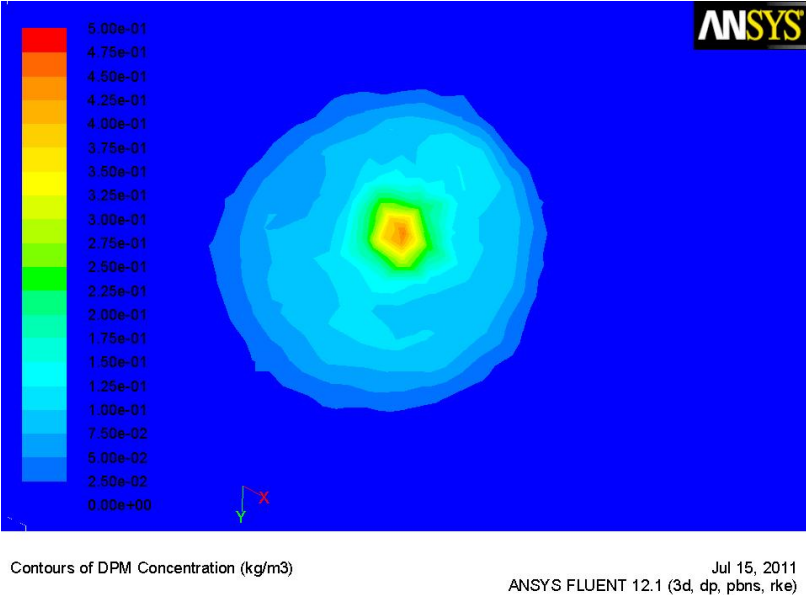


Figure A.1: Contours of DPM Concentration - Baseline Condition

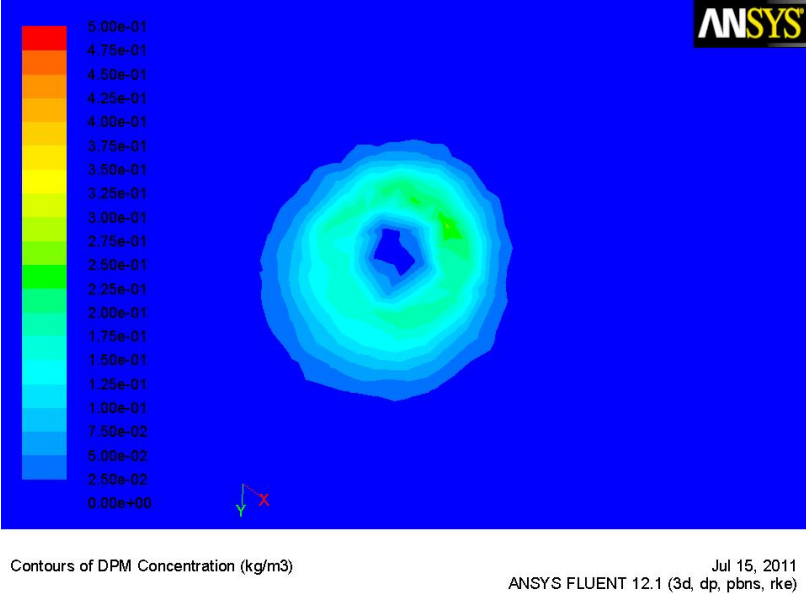


Figure A.2: Contours of DPM Concentration - Condition Reducing the in Initial Spray Angle By 10%

APPENDIX A. CONCENTRATION PLOTS CREATED ON A PLANE 1.5 INCHES FROM THE NOZZLE FACE

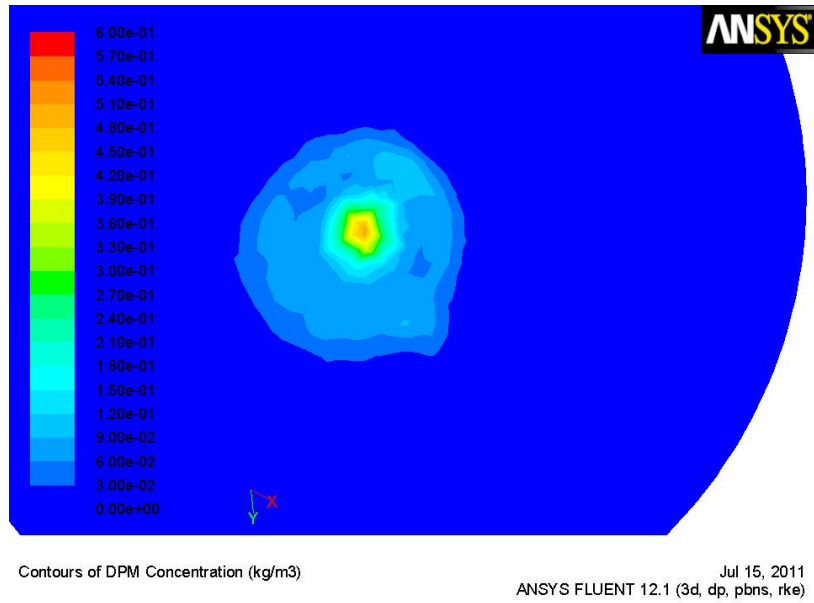


Figure A.3: Contours of DPM Concentration - The Rosin-Rammler Number of Classes Parameter

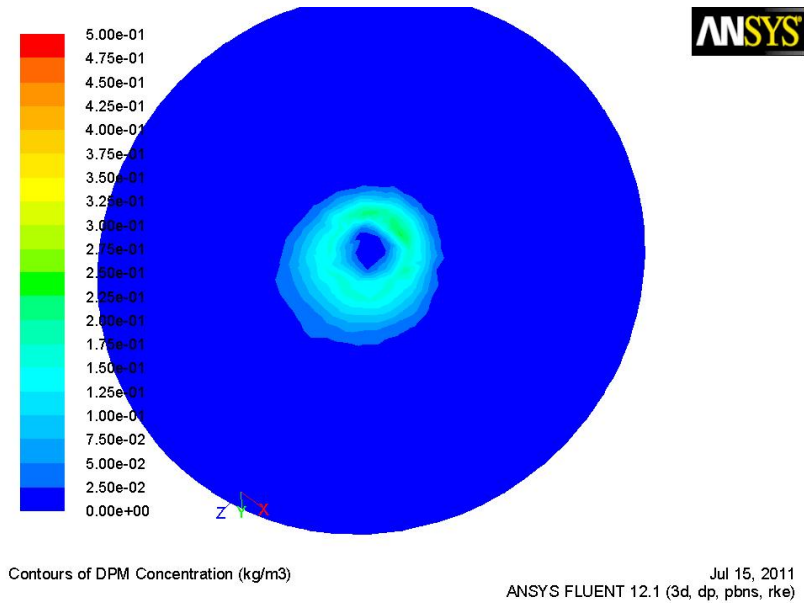
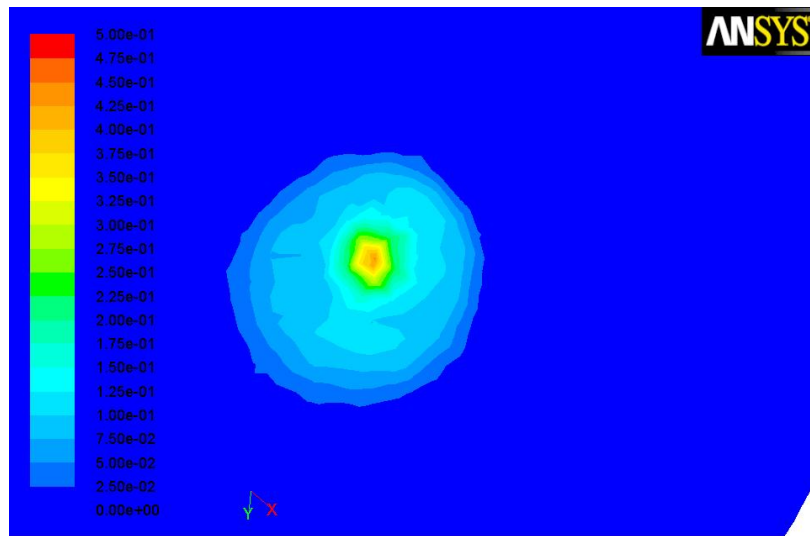


Figure A.4: Contours of DPM Concentration - Condition Increasing the Initial Spray Angle By 10%



Contours of DPM Concentration (kg/m3)

Jul 15, 2011
ANSYS FLUENT 12.1 (3d, dp, pbns, rke)

Figure A.5: Contours of DPM Concentration - The Rosin-Rammler Spread Parameter

References

- [1] K Adiga and R Hatcher. A computational and experimental study of ultra fine water mist as a total flooding agent. *Fire Safety Journal*, Jan 2007.
- [2] ANSYS INC, 275 Technology Drive Canonburg, PA. *ANSYS FLUENT Getting Started Guide*, 13 edition, November 2010.
- [3] ANSYS Inc., 275 Technology Drive Canonburg, PA. *Ansys FLUENT Theory Guide*, 13.0 edition, November 2010.
- [4] ANSYS Inc., 275 Technology Drive Canonburg, PA. *ANSYS FLUENT User's Guide*, 13.0 edition, November 2010.
- [5] ANSYS Inc, 275 Technology Drive Canonburg, PA. *User Manual*, ansys icem cfd 13.0 edition, November 2010.
- [6] Nicolas E Antoine and Ilan M Kroo. Framework for aircraft conceptual design and environmental performance studies. *AIAA Journal*, Jan 2005.
- [7] S. V. Sankar W.D. Bachalo. Response characteristics of the phase doppler particle analyzer for sizing spherical particles larger than the light wavelength. *Applied Optics*, 30(12):1487–1496, 1991.
- [8] Arthur H. Lefebvre Dilip R. Ballal. *Gas Turbine Combustion Alternative Fuels and Emissions*. CRC Press Taylor and Francis Group, third edition, 2010.
- [9] G Blokkeel, A Mura, and F Demoulin. . . . A continuous modeling approach for describing the atomization process from inside the injector to the final spray. . . . *Atomization and Spray . . .*, Jan 2003.

-
- [10] R. O. Brodkey. *The Phenomena of Fluid Motions*. Addison-Wesley, 1967.
- [11] P DesJardin and L Gritz. A dilute spray model for fire simulations: formulation, usage and benchmark problems. *osti.gov*, Jan 2002.
- [12] Fluent Inc, 10 Cavendish Court Lebanon, NH 03766. *FLUENT 6.3 User's Guide*, September 2006.
- [13] MG Giridharan, D S Crocker, J Widmann, and C Presser. Issues related to spray combustion modeling validation. In *AIAA 39th Aerospace Sciences Meeting and Exhibit*, pages 1–9. American Institute of Aeronautics and Astronautics, January 2001.
- [14] M. Sommerfeld H. Qiu. A reliable method for determining the measurement volume size and particle mass fluxes using phase-doppler anemometry. *Experiments in Fluids*, 13(6):393–404, 1992.
- [15] J. O. Hinze. Fundamentals of the hydrodynamic mechanism of splitting in dispersion processes. *AIChE Journal*, 1(33):289–295, 1995.
- [16] S Kamnis. 3-d modelling of kerosene-fuelled hvof thermal spray gun. *Chemical Engineering Science*, Jan 2006.
- [17] S Kamnis. Numerical modelling of propane combustion in a high velocity oxygen-fuel thermal spray gun. *Chemical Engineering and Processing*, Jan 2006.
- [18] M. Sevik S. H. Park. The splitting of drops and bubbles by turbulent fluid flows. *Journal of Fluids Engineering*, 95:53–60, 1973.
- [19] Pratt and Whitney Canada. Pwc request for test at national research council of canada document.
- [20] C.D Rakopoulos, K.A Antonopoulos, D.C Rakopoulos, and D.T Hountalas. Multi-zone modeling of combustion and emissions formation in di diesel engine operating on ethanol-diesel fuel blends. *Energy Conversion and . . .*, Jan 2008.
- [21] L Rayleigh. On the instability of jets. *Proceedings of London Mathematical Society*, 10:4–13, 1878.

-
- [22] J Kirwan S Das, S Chang. Spray pattern recognition for multi-hole gasoline direct injectors using cfd modeling. *SAE Technical Paper*, Jan 2009.
- [23] William A. Sirignano. *Fluid Dynamics and Transport of Droplets and Sprays*. Cambridge, second edition, 2010.
- [24] SIBENDU SOM. *Development and Validation of Spray Models for Investigating Diesel Engine Combustion and Emissions*. PhD thesis, University of Illinois at Chicago, 2009.
- [25] G Sturgess, S Syed, and K McManus. Calculation of a hollow-cone liquid spray in a uniform airstream. *Journal of Propulsion and . . .*, Jan 1985.
- [26] C. Weber. Disintegration of liquid jets. *Zeitschrift fur Angewandte Mathematik und Mechanik*, 11(2):136–159, 1931.

